ECOLOGY | ARTICLE

The effect of single versus successive warm summers on an intertidal community

Amelia V. Hesketh[1,2*], Cassandra A. Konecny[2], Sandra Emry[2], and Christopher D. G. Harley[2,3]

Author affiliations:

1. School of Resource and Environmental Management, Simon Fraser University, Burnaby, BC, Canada
2. Department of Zoology, University of British Columbia, Vancouver, BC, Canada
3. Institute for the Oceans and Fisheries, University of British Columbia, Vancouver, BC, Canada

* Corresponding author: ahesketh@sfu.ca

OPEN RESEARCH STATEMENT:

Data are archived in Zenodo: https://doi.org/10.5281/zenodo.15054128. Code is also archived in Zenodo: https://doi.org/10.5281/zenodo.15054111.

KEYWORDS: barnacles; climate change; community; diversity; foundation species; heatwaves; intertidal zone; mortality; repeated stressors; warming

ABSTRACT

To accurately predict how organisms and ecological communities will respond to future conditions caused by climate change, we must consider the temporal dynamics of environmental stressors, including the effects of repeated exposures to stress. We performed a two-year passive thermal manipulation in coastal British Columbia, Canada to determine how intertidal communities responded to single and successive warm summers. Warm temperatures had both negative contemporaneous effects within years and persistent negative effects across years. Warming reduced organism densities, altered population dynamics, and affected community structure and diversity, patterns which were likely mediated by differences in foundation species (barnacle) abundance between treatments. Unexpectedly, the effects of thermal stress in the second year were rarely dependent on whether temperatures were warm during the first year. Our study suggests that, while this intertidal community can recover from single warm summers, recurring thermal stress has additive negative effects, resulting in a more depauperate, less diverse community over time, particularly if foundation species are negatively affected.

INTRODUCTION

Just as global mean surface temperatures are expected to increase over the coming decades (IPCC 2023), so, too, are the frequency, severity, and duration of extreme temperature events such as heatwaves (Oliver et al. 2018, Perkins-Kirkpatrick and Lewis 2020). Extreme temperatures have biological consequences. Heatwaves increase the probability of environmental temperatures surpassing the thermal optima and maxima of organisms (Vasseur et al. 2014). Thus, heatwaves can impair fitness (Siegle et al. 2022) and, ultimately, cause mortality for thermally sensitive species (Harley 2008, Hesketh and Harley 2023), with ramifications for

47 populations, communities, and ecosystems (Harris et al. 2018; Montie and Thomsen 2023).
48 The effects of heatwaves on organisms are increasingly well-studied; however, the
49 consequences of repeated exposures to thermal stress have received less attention. Thermal stress
50 events that are prolonged or occur in rapid succession can exert stronger negative effects on
51 organism survival and fitness (Ma et al. 2018; Siegle et al. 2022). However, responses vary
52 among species — for species with acclimatory capacity, prior exposure to thermal stress may
53 engender resilience to subsequent heatwaves, while for those without, the negative effects of
54 repeated heatwaves may instead accumulate (Pansch et al. 2018). At the community level, for
55 which controlled warming manipulations can be experimentally challenging and studies are
56 correspondingly limited, repeated heatwaves have resulted in communities that are more
57 depauperate (Dal Bello et al. 2019) and homogenous (Hammill and Dart 2022). However,
58 community-level resilience to thermal stress may increase with repeated exposures as thermally
59 sensitive species are eliminated and thermally tolerant species survive (Hughes et al. 2019).
60 Manipulating the timing of thermal stress events is an important additional step towards
61 understanding their ecological effects.
62 While environmental extremes affect organisms, the reverse is also true. Foundation
63 species, abundant species that physically structure ecological communities, often create
64 environmentally benign microhabitats for associated organisms (e.g., through moisture retention
65 and shading; Hesketh et al. 2021, Lee et al. 2021, Jurgens et al. 2022, Gutiérrez et al. 2023). The
66 loss of foundation species can thus profoundly impact communities by disrupting interspecific
67 facilitative relationships (Hesketh and Harley 2023; Montie and Thomsen 2023). The importance
68 of such facultative facilitations for bolstering organism survival and performance often increases
69 with environmental stress, though there may be an upper limit beyond which stress cannot be

effectively buffered (Bulleri et al. 2016).

Intertidal organisms are regularly exposed to stressors including hydrodynamic forces, desiccation, and seasonally hot and cold air temperatures. In this highly variable, physiologically taxing environment, foundation species may play an outsized role in attenuating stress and supporting biodiversity. While many intertidal species act as foundation species (e.g., bed-forming bivalves, tunicates, macroalgae, and vascular plants), here, we focus on acorn barnacles. Acorn barnacles are cosmopolitan organisms that facilitate a relatively diverse intertidal community (Harley 2006, Hesketh et al. 2021). Barnacles can retain moisture (Vermeij 1978, Harley and O'Riley 2011), thereby reducing desiccation stress for closely associated species when present at high densities. However, thermal stress can increase barnacle mortality and reduce barnacle abundance (Little et al. 2021; Hesketh and Harley 2023). While empty barnacle tests provide humid, thermally benign microhabitats for other species (Barnes 2000), such habitats are ultimately ephemeral. Barnacle mortality events and recruitment failures, by reducing available habitat, significantly impact the abundance, identity, and diversity of associated organisms (Kordas et al. 2015, Hesketh and Harley 2023).

Here, we tested the effect of single and successive warm summers on high intertidal barnacle bed communities (Fig. 1a) through a two-year passive thermal manipulation using black (warm) and white (cool) settlement tiles (Fig. 1b; Kordas et al. 2015). To manipulate the temporal dimension of thermal stress, the treatments (color) of half of the tiles were swapped after one year. We hypothesized that: H1) because elevated temperatures can reduce organism performance and increase mortality, communities within the warm treatments would have lower invertebrate abundance, algal cover, and alpha diversity than those within cool treatments; H2) warming during the first year, because of its negative contemporaneous effects on foundation

93 species cover, would exert persistent indirect negative effects during the second year; and H3)
94 the effects of warming in the second year of study would be stronger in communities that were
95 previously exposed to warming due to pre-existing reductions in foundation species cover, and
96 thus reduced availability of thermal refugia (i.e., a positive interaction of warming across years;
97 Fig 1b).
98
99 **MATERIALS AND METHODS**
100 *Site description*
101 This study was completed near T̓ESNO ̓EN̲ (Beaver Point), a site that lies within the
102 traditional, unceded territory of the W̱SÁNEĆ peoples in what is now known as Ruckle
103 Provincial Park on Salt Spring Island, British Columbia, Canada (48.77324, -123.36637). The
104 substratum at this site is dominated by a southeast-facing semi-exposed sandstone bench, and
105 tides are mixed semi-diurnal. Relative to the rest of British Columbia's Southern Gulf Islands,
106 this area is exposed to cooler, more saline water and larger waves due to its proximity to Haro
107 Strait and the Strait of Juan de Fuca. However, like these and the neighboring San Juan Islands
108 (USA), the intertidal zone at this site is considered a thermal "hot spot" due to its summertime
109 midday low tides coupled with relatively clear, sunny weather (Helmuth et al. 2006).
110 Here, the upper intertidal zone is dominated by the acorn barnacles *Balanus glandula* and
111 *Chthamalus dalli*, with sporadic beds of the perennial brown alga *Fucus distichus*. Filamentous
112 ephemeral algae (predominantly the green algae *Ulothrix* sp. and *Urospora* sp.) occur as early
113 colonizers of bare space and foliose ephemeral algae (predominantly *Ulva* spp., *Pyropia* sp., and
114 *Petalonia fascia*) occur in winter, often attached to underlying barnacles. Dominant herbivores
115 include the littorine snails *Littorina scutulata* and *Littorina sitkana* and the limpets *Lottia*

116 *paradigitalis* and *Lottia digitalis*, which tend to migrate down shore with the onset of daytime
117 low tides in spring and return to higher tidal elevations in August (Kordas et al. 2015).
118
119 *Study design*
120 Individual settlement tiles were built based on previous methods (Kordas et al., 2015; see
121 Appendix S1). In brief, each 15x15 cm tile consisted of a central epoxy settlement surface
122 (6.9x6.9 cm, < 5 mm high Sea Goin' Poxy Putty; Permalite Plastics, USA) bordered by either
123 white (cool treatment) or black (warm treatment) high-density polyethylene (6.4 mm thick;
124 Redwood Plastics, Canada). Temperature differences were driven by the differential absorption
125 of incoming solar radiation during daytime summer low tides. These settlement tiles were affixed
126 to a bottom tile unit composed of thicker white high-density polyethylene (9.5 mm thick;
127 Redwood Plastics, Canada) that was used to anchor the assembly to the underlying bedrock.
128 This study followed a randomized block design, with six blocks consisting of eight black
129 and eight white tiles (n = 48). Tiles were initially installed on 12 April 2019. Some were
130 relocated in June 2019 to avoid disturbance from wave-cast logs, resulting in a final shore level
131 of 2.34 ± 0.07 m (mean ± SE) above Canadian chart datum. In May 2019, we enclosed tiles with
132 copper "fences" to manipulate grazer diversity and densities (see Appendix S1). We ceased
133 manipulations in August 2019 because wave action, moreso than we, controlled littorine snail
134 densities and high summer temperatures caused mortality for limpets, which were prevented
135 from accessing thermal refugia by copper fences. On 3 April 2020, we randomly selected and
136 switched the colour of half of each treatment within each block using white and black heavy-
137 duty tape (Gorilla Tape; Gorilla Glue, Inc., USA; adhesion enhanced with LePage Ultra Gel
138 super glue). This change created four thermal history treatments during the second year (cool

139 summer–cool summer, CC; cool–warm, CW; warm–cool, WC; and warm–warm, WW; n = 24).
140 Sample sizes varied over time due to tile damage and dislodgement (Appendix S1: Fig. S3).
141
142 *Temperature measurements*
143 For small ectotherms with a large area of attachment to the substratum (e.g., barnacles),
144 substratum temperature is a reasonably good proxy for body temperature (Kordas et al. 2015).
145 Thus, the substratum temperature of both settlement tiles and adjacent bedrock were collected
146 using pre-programmed iButton temperature loggers (model DS1921G-F5# Thermochron, Dallas
147 Semiconductor, USA). To record tile temperature, loggers were sealed in nitrile pouches and
148 sandwiched between the two plates of experimental tile units. To record bedrock temperature,
149 loggers were wrapped in Parafilm and affixed to shore with a 2–3 mm layer of A–788 Splash
150 Zone epoxy (Pettit Paints, USA) separating the logger from both the underlying shore and
151 surrounding air. The number of loggers recording within each treatment varied through time due
152 to changes in the number of treatment groups between years and instrument failure.
153 Temperatures were recorded hourly except over the second winter of the study, when
154 temperatures were instead recorded every two hours.
155
156 *Community surveys*
157 We characterized organism abundance and community diversity through regular visual
158 surveys of tiles and destructive sampling at the end of the study. Visual surveys occurred
159 approximately monthly during summer and every two months during winter from 8 May 2019 to
160 24 February 2021. During surveys, each invertebrate species was counted and the percent cover
161 of each algal species was recorded. Organisms were identified to species except for amphipods

and isopods, which were identified to order, and diatom mats, which were lumped into one taxon. Sessile species were only recorded within the central 6.4 × 6.4 cm area of the epoxy settlement surface using a wire mesh quadrat (mesh size = 6.4 mm × 6.4 mm) to avoid edge effects. Any sessile species growing on the colored tile borders were removed during surveys. Motile invertebrates were counted on the entire tile surface, including on colored tile borders where their influence on the experimental community could not be ruled out. We destructively sampled half of the tiles within each treatment and block on 14 September 2020 (permanently removing these from the study) and sampled remaining tiles on 24 February 2021, scraping all biota from the settlement surface into containers of 70% ethanol (v/v in water). Epifauna were identified and counted under a dissecting microscope. Intertidal organisms were collected under Fisheries and Oceans Canada scientific collection permits (XR 61 2019 and XR 196 2020).

Statistical analyses

We used linear mixed effects models, constructed with *glmmTMB* (Brooks et al. 2017), to test for differences in mean daily maximum (MDM) temperature between treatments. Because of frequent logger failures, temperature records for individual tiles were often incomplete, potentially biasing data. Thus, we imputed missing hourly temperatures with the *mice* package (van Buuren and Groothuis-Oudshoorn 2011) for all bedrock temperature records and the two most complete tile records per year two treatment in each block (i.e, for bedrock, N=6 and for tiles N=12 in year two, N=24 in year one). Data from each year were imputed separately using five iterations with the classification and regression trees method, with hourly ERA5 satellite-derived 2m surface temperature (Hersbach et al. 2023) used as an auxiliary variable. The resulting set of imputations was averaged. Because differences were driven by solar irradiance,

temperature data were retained only if they were collected during daytime summer low tides (1 May – 31 August; see Appendix S1 for details), when treatment differences were likely strongest. Calculated MDM temperatures were modeled as a function of treatment. Random intercept effects of individual tile and date were included, the latter with an AR(1) process to account for autocorrelation.

We tested how temperature treatments affected barnacle recruitment and abundance, grazer abundance, and alpha diversity using generalized linear models with *glmmTMB* (Brooks et al. 2017). Differences in barnacle recruitment between treatments were evaluated during peak recruitment (May or June), while differences in adult abundance were evaluated in winter when spring recruits had reached maturity. Grazer abundance and community diversity were evaluated at the end of summer to characterize the immediate effects of heat stress and again in late winter to allow an opportunity for community recovery. During the first year, responses were modeled as a function of the treatment (cool or warm), while during the second year, they were modeled as a function of the factorial combination of year one treatment and year two treatment. Experimental block was included as a random effect. A fixed effect for original grazer treatments (see details in Appendix S1) was initially included in models of data collected from 8 May 2019 until September 2020, one year after manipulations ceased. If this term was significant, data were not analyzed (true for algal Shannon diversity and cover in year one); if this term was not significant, then it was dropped from the model. Grazer abundance data collected prior to September 2020 were not modeled due to initial grazer community manipulations. Model assumptions were checked using the *DHARMa* package (Hartig 2022). Species richness was log-transformed in for the post-summer timepoint in year two to ensure the model met assumptions. *P*-values were calculated using the Anova function within the *car* package (Fox and Weisberg

208 2019) with a significance threshold of $P = 0.05$. We also chose to use multiple comparisons tests
209 (Tukey-Kramer *post hoc* tests) to detect differences between treatment combinations because we
210 expected the consistently warm treatment to have substantially different structure than other
211 treatments (Hypothesis 3). For these tests, we used the *emmeans* package (Lenth 2022).

212 Given the complex and, at times, opposite effects of temperature on algal cover over
213 time, we used generalized additive modeling with the *mgcv* package (Wood 2011) to analyze
214 how temperature affected algal cover dynamics during each year. Within these autoregressive
215 AR(1) models, we included linear terms — for year one, treatment alone, and for year two, an
216 factorial combination of treatments in year one and year two — smooth terms of time (days since
217 the experiment start) for each treatment, and a random effect of block. Pairwise differences in
218 algal cover over time between control treatments (C or CC) and other treatments were calculated
219 and visualized using the methods of Rose et al. (2012). Early grazer manipulations exerted a
220 significant effect on algal cover during the first year, and thus survey data collected during the
221 first year were excluded from analysis.

222 Treatment-driven differences in epifaunal community structure and beta diversity were
223 modeled with the *vegan* package (Oksanen et al. 2020) for communities immediately following
224 summer heat stress and after winter recovery in the second year of study. Data were ordinated
225 using distance-based redundancy analysis with Bray-Curtis distances. Community structure was
226 modeled as a function of the interaction of treatment in year one and year two using
227 PERMANOVA analyses with 9999 permutations constrained within experimental blocks.
228 Multiple pairwise comparisons were made with *multiconstrained* in the *BiodiversityR* package
229 (Kindt and Coe 2005). Beta diversity was modeled as a function of treatment using PERMDISP
230 analyses with bias adjustment for small sample sizes.

To reflect our underlying analyses, results are subsequently reported by response variable. We relate patterns in each biological response to our initial hypotheses (H1–H3) in Appendix S1: Table S3 and report all the statistical outputs of our models in Appendix S2.

RESULTS

Differences in substratum temperature

Substratum temperatures differed significantly among the cool treatment (white tiles), warm treatment (black tiles), and adjacent bedrock during daytime low tides from May through August. Mean daily maximum (MDM) summer temperatures were consistently ~2 ºC higher in warm versus cool treatments (Appendix S1: Table S2), with a grand mean of 29.2 ± 7.0 ºC across all warm treatments and 27.1 ± 6.4 ºC across all cool treatments. Meanwhile, bedrock was 28.5 ± 7.0 ºC during the first summer and 28.1 ± 6.4 ºC during the second summer. During the first summer, both the warm treatment and bedrock had significantly higher MDM temperatures than the cool treatment (Figure 2; ANOVA: $\chi^2_2 = 40.53$, $P < 0.001$; Appendix S2: Tables S1–2). During the second summer, warm treatments had significantly higher MDM temperatures than cool treatments, with bedrock temperatures intermediate and statistically similar to all other treatments (ANOVA: $\chi^2_4 = 52.34$, $P < 0.001$; Appendix S2: Tables S3–4). During the second year, taped tile surfaces effectively mimicked the treatment effect of bare tile surfaces (i.e., WC and CW had analogous MDM temperatures to CC and WW, respectively; Appendix S2: Table S7). Mean substratum temperatures displayed analogous patterns to MDM temperatures (Appendix S1: Table S3; Fig. S5; Appendix S2: Tables S5–8).

Effects on barnacle recruitment and abundance

Warm summer temperatures tended to reduce the abundance of barnacle recruits. When peak recruitment was observed during the first year (May and June, respectively, for *B. glandula* and *C. dalli*), temperature treatment did not significantly affect *B. glandula* recruitment (Fig. 3a; Appendix S2: Table S9), but *C. dalli* recruitment was lower within the warm treatment (Fig. 3b; Type II ANOVA, χ^2_1= 4.13, P = 0.0422; Appendix S2: Table S10). Warming had both contemporaneous and carry-over effects on barnacle recruitment during the peak recruitment window of the second year (June for both species). Fewer *Balanus glandula* were present in warm treatments, whether warming occurred during the second summer (Type III ANOVA, treatment_{y2}; χ^2_1=38.34, $P < 0.001$; Appendix S2: Tables S11–12) or during the first summer (treatment_{y1}; χ^2_1=6.07, P = 0.0138). The recruitment of *C. dalli* in year two was similarly negatively affected by warming in both years (Fig. 3b; Type III ANOVA; treatment_{y2}: χ^2_1=19.16, $P < 0.001$; treatment_{y1}: χ^2_1=5.56, P = 0.0184; Appendix S2: Tables S13–14).

Warming reduced the abundance of adult *B. glandula*, but not adult *C. dalli*. At the end of the first winter, there were substantially fewer adult *B. glandula* in the warm treatment (Fig. 3c; Type II ANOVA; χ^2_1=106.20, $P < 0.001$; Appendix S2: Table S15). At the end of the study, *B. glandula* abundance appeared to be lower where warming was applied in both summers, but this trend lacked significant statistical support (Type III ANOVA; $P \sim 0.1$ for treatment_{y1} and treatment_{y2}; Appendix S2: Table S16). However, *post hoc* testing suggested that *B. glandula* was more abundant in the consistently cool treatment compared to the consistently warm treatment (Tukey-Kramer; z ratio = 3.08, P = 0.0111; Appendix S2: Table S17). During summer in both years, the mortality of *B. glandula* was higher and surviving barnacles were smaller within warm treatments (Appendix S1: Fig. S7–8; Appendix S2: Tables S18–21). The abundance of adult *C. dalli* was similar between treatments in both years (Fig, 3d; Appendix S2: Tables S22–24).

277

278 *Effects on grazer abundance*

279 During the second year of study, grazer abundance was negatively correlated with
280 warming. Warming had a contemporaneous effect on limpet abundance (Fig. 4a), both
281 immediately following summer (September 2020; Type III ANOVA; $\chi^2_1 = 11.07$, $P < 0.001$;
282 Appendix S2: Tables S25–26) and at the end of winter (February 2021; Type III ANOVA; $\chi^2_1 =$
283 3.87, $P = 0.0491$; Appendix S2: Tables S26–27). Post-summer littorine snail abundance was
284 lower in warm treatments, whether warming was applied during the first or second summer (Fig.
285 4b; Type III ANOVA; treatment_{y1}: $\chi^2_1 = 17.56$, $P < 0.001$; treatment_{y2}: $\chi^2_1 = 13.38$, $P < 0.001$;
286 Appendix S2: Tables S28–29). Similar trends in littorine snail abundance were observed at the
287 end of winter, though with reduced statistical support (Type III ANOVA; treatment_{y1}: $\chi^2_1 = 3.29$,
288 $P = 0.0698$; treatment_{y2}: $\chi^2_1 = 3.87$, $P = 0.0491$; Appendix S2: Tables S30–31).

289

290 *Effects on algal cover*

291 Algal cover and the timing of algal blooms differed between treatments, particularly in
292 the first year of study (Fig. 5a-b). Algal cover reached a similar maximum between treatments,
293 driven by a bloom of the green ephemeral alga *Ulothrix* sp. near the end of the first summer.
294 However, the temporal dynamics of algal cover differed between treatments; cover peaked
295 earlier and declined more rapidly within the cool treatment relative to the warm treatment. After
296 ineffectual grazer manipulations were abandoned during the first year, algal cover in the warm
297 treatment remained significantly higher than in the cool treatment until winter (Fig. 5b; *gamm*; t
298 = 3.30, $P = 0.00109$; Appendix S2: Table S32). During the second year, algal cover remained
299 relatively low, but was higher in treatments that alternated thermal conditions relative to those

300 that were consistently cool or warm (*gamm*; t = -2.57, $P = 0.0104$; Appendix S2: Table S33).

301

302 *Effects on diversity*

303 Warming tended to reduce alpha diversity and alter community structure, particularly in
304 communities that experienced successive warm summers. During the first year, species richness
305 was lower in the warm treatment, whether richness was assessed immediately after summer (Fig.
306 6a; Type II ANOVA; $\chi^2_1=16.33$, $P < 0.001$; Appendix S2: Table S34) or at the end of winter
307 (Type II ANOVA; $\chi^2_1=74.85$, $P < 0.001$; Appendix S2: Table S35). During the second year,
308 post-summer species richness was lower in treatments that experienced contemporaneous
309 warming (Fig. 6b; Type III ANOVA; $\chi^2_1=4.73$, $P = 0.0297$; Appendix S2: Tables S36–37), but
310 were unaffected by warming applied in the first year. After winter recovery, no overall effect of
311 temperature treatment in either summer was discernible (Appendix S2: Table S38), but *post hoc*
312 pairwise comparisons suggested that the treatment that was successively warmed had lower
313 diversity than treatments that were cool during the second summer (Appendix S2: Table S39;
314 Tukey-Kramer; CC–WW: z ratio = 3.87, $P < 0.0001$; WC–WW: z ratio = 3.27, $P = 0.00590$).
315 Warming also exerted a negative effect on the Shannon diversity of the invertebrate community;
316 during winter of the first year, diversity was significantly lower within the warm treatment, and
317 during the second year, diversity was lower in treatments where warming was applied during the
318 first year (Appendix S1: Fig. S11a–b, Appendix S2: Tables S40–45). The Shannon diversity of
319 the algal community, meanwhile, was reduced by warm temperatures during the first year, but
320 not affected during the second year (Appendix S1: Fig. S11c, Appendix S2: Tables S46–48).
321 Epifaunal communities characterized on destructively sampled tiles demonstrated that
322 community structure, but not beta diversity, differed between treatments. At the end of the

second summer (September 2020; Fig. 6c), there were no significant differences in community structure between treatments based on PERMANOVA (Appendix S2: Table S49), though *post hoc* pairwise comparisons indicated the CC and WW treatments differed in composition (Appendix S2: Table S50; *multiconstrained*; $F_1 = 2.68$, $P = 0.018$). At the end of the experiment (February 2021; Fig. 6d), however, warm temperatures in year one and year two interacted to drive differences in community structure (PERMANOVA; $F_{1,37} = 2.22$, $P = 0.0125$; Appendix S2: Table S51). *Post hoc* comparisons showed that this was primarily driven by differences between the structure of the consistently cool treatment and all others (Appendix S2: Table S52). Beta diversity was similar among treatments (Appendix S2: Tables S53–54). The alpha diversity of these epifaunal communities was generally lowest in the consistently warm treatment, particularly compared with samples where temperatures were cool during the second summer (Appendix S1: Figure S12; Appendix S2: Tables S55–62).

DISCUSSION

In this study, we passively manipulated the substratum temperature of intertidal settlement tiles over two consecutive summers to determine the effects of present and past warming and whether prior thermal stress influences the impact of subsequent thermal stress. We expected that warming would have contemporaneous direct negative effects on organism abundance and diversity (H1) and persistent indirect negative effects mediated by lower foundation species cover (H2). We expected that warming during the second year would have greater negative effects where conditions were previously warm, since foundation species cover and thus thermal refugia would be constrained, thereby increasing stress for associated biota (H3). As anticipated, we found that warming often had both contemporaneous and persistent

346 negative effects on organism abundance and community alpha diversity, though its effects on
347 algae were more complex. Contrary to our prediction, the magnitude of the effects of warming in
348 the second summer were usually independent of whether warming had been previously applied.
349 The methodology employed in this study was effective in manipulating substratum
350 temperatures. In both years, the surfaces of white tiles were cooler than those of black tiles, as in
351 previous studies (Kordas et al. 2015, 2017). Interestingly, bedrock temperatures were more
352 analogous to those of black tiles during the first year. This unexpected pattern could be an
353 artefact of shading from copper fences that encircled tiles for most of the first summer, but not
354 the second, which may have artificially cooled tile surfaces relative to adjacent bedrock. The
355 intermediate temperatures of bedrock recorded in the second year of study may reflect its grey
356 color, which absorbs more solar insolation than a purely white surface, but reflects more solar
357 insolation than a purely black surface. Regardless of trends in bedrock temperature, the
358 temperatures of white (cool) and black (warm) tiles and the degree of difference between them
359 were consistent across years, which drove corresponding biological differences.
360 The recruitment and abundance of acorn barnacle foundation species (*B. glandula* and *C.*
361 *dalli*) was typically lower within warm treatments, consistent with past studies (Kordas et al.
362 2015, 2017, Kordas and Harley 2016). For *B. glandula*, the dominant barnacle in this system, the
363 highest recorded LT_{50} in air is 43 ºC (Hamilton and Gosselin 2020), though mortality has been
364 observed at 40 ºC (Ober et al. 2019). Substratum temperatures within all treatments exceeded
365 these lethal thresholds during daytime summer low tides, with warm treatments reaching 45 ºC
366 during both years. While barnacles tend to remain slightly cooler than surrounding bedrock
367 (Harley and Lopez 2003), the higher mortality we observed for *B. glandula* within warm
368 treatments suggest that barnacle body temperatures, particularly on black tiles, exceeded critical

thermal limits. Even exposure to sublethal temperatures can incur metabolic costs; high temperatures can impair *B. glandula* respiration for many hours after exposure (Ober et al. 2019), and sustained warm temperatures can slow barnacle growth (Kordas and Harley 2016). Here, *B. glandula* tended to be smaller within warm treatments, indicating that surviving barnacles experienced sublethal thermal stress that impaired growth. The tendency of barnacles to settle gregariously may magnify direct negative effects on abundance and recruitment if warming is sustained. Barnacles preferentially recruit to areas containing conspecifics, a strategy that increases the likelihood of successful sexual reproduction via internal fertilization (Wu 1981). Thus, recruitment to previously warm tiles during the second year may have been lower because these tiles hosted fewer adult barnacles. The other acorn barnacle present, *C. dalli*, was not prevalent during the first year, possibly due to interannual variation in recruitment dynamics common in barnacles (Scrosati and Ellrich 2016). Recruitment in the second year was lower within warm treatments, but adult abundance was unaffected by treatment, possibly because adult *C. dalli* are more robust to thermal stress than *B. glandula*, with an LT_{50} near 44.5 ºC (Hamilton and Gosselin 2020). Grazer manipulations during the first summer may have reduced barnacle recruitment and hampered the detection of a treatment effect, since limpets, which were purposefully included or excluded from both white and black tiles, are known to remove barnacle recruits during grazing (Dayton 1971).

During the second year, reduced grazer abundance in the warm treatments may have been due to the direct effects of temperature and/or indirect effects mediated by differences in barnacle abundance. One common limpet in this system, *Lottia digitalis*, has an upper thermal limit of 38 ºC in air (Bjelde and Todgham 2013). High intertidal littorine snails have a slightly greater tolerance to elevated temperatures (41.01 ºC for *L. sitkana* and 41.47 ºC for *L. scutulata*

during five-hour emersions; Stickle et al. 2017). While these dominant grazers are thermally robust, recorded summer substratum temperatures frequently exceeded these thresholds for short periods. Temperatures likely regularly fluctuated above grazer thermal optima (e.g., 30 ºC for *L. digitalis*; Bjelde and Todgham 2013), which could have suppressed grazer activity, and thus foraging effectiveness (Rickards and Boulding 2015). Motile organisms can behaviourally thermoregulate by moving to avoid thermal stress. Grazers were not commonly observed on tiles during the summer, though surveys occurred exclusively at low tide, when some grazers avoid feeding (Little 1989), and we may have thus underestimated abundance. However, these temporal dynamics suggest that, while warm temperatures may have directly reduced grazer abundance, indirect effects are more likely. Limpets and littorine snails were generally more abundant within cool treatments where barnacle cover was higher, a pattern consistent with other studies (Silva et al. 2015, Hesketh et al. 2021). Barnacles can reduce desiccation stress for associated species by creating moist, humid microhabitats during low tides (Vermeij 1978; Harley and O'Riley 2011); thus, the abundant, larger barnacles present on cool tiles may have generated a higher density of favorable microhabitats, begetting a higher abundance of grazers.

Barnacles, in addition to providing microhabitats, may have influenced grazer abundance through their effects on algal food supply. The green filamentous *Ulothrix* sp. initially dominated bare tiles, but eventually declined and was replaced by other foliose algal species — usually growing on barnacle tests — a pattern observed in past studies (Kordas et al. 2017). While maximum algal cover was similar between temperature treatments during the first year, its temporal dynamics differed; algal cover peaked later and declined more slowly within the warm treatment. High temperatures can have highly variable interspecific effects on algae (Kordas et al., 2017). *Ulothrix* sp. may have thrived under warm summer conditions due to higher growth

415 rates, because grazer activity was suppressed by high temperatures, or because barnacles, which
416 can compete with algae for space or harbor populations of voracious grazers (Hesketh et al.
417 2021), were less abundant and smaller. On adjacent bedrock, *Ulothrix* sp. was most commonly
418 observed in bare, log-damaged patches within barnacle beds, supporting an indirect negative
419 effect of barnacles on this species (as has been documented with the ephemeral green alga
420 *Urospora* spp.; Harley 2006). Meanwhile, other algae (here, *Pyropia* sp. and *Ulva* sp.) may
421 preferentially attach to rugose barnacle tests, and barnacles can provide refuge from desiccation
422 and grazing (particularly by limpets) for algal spores and germlings (Farrell 1991; Geller 1991).
423 Thus, algal cover may have been highest in the warm-cool and cool–warm treatments during the
424 second year because shifting thermal conditions created a heterogenous mixture of bare space
425 and sparse barnacles, allowing for the growth of both desiccation-tolerant, barnacle-phobic and
426 desiccation-intolerant, barnacle-philic algae.
427 Thermal stress, by shaping barnacle, grazer, and algal populations, had higher-level
428 impacts on diversity and community structure. Alpha diversity generally increased over the
429 course of succession but remained lower in warm treatments, as has been found previously
430 (Kordas et al. 2015, Kordas et al. 2017). Barnacle recruits, followed by opportunistic ephemeral
431 algae, appeared shortly after tiles were installed, consistent with studies involving intertidal
432 disturbance and succession in the northeast Pacific (Farrell 1991, Geller 1991). Because
433 barnacles act as both facilitators (Farrell 1991) and food sources (Harley and O'Riley 2011)
434 within the high intertidal zone, their presence allowed grazers (e.g., amphipods, limpets),
435 secondary successional species (e.g., perennial algae), and predators (e.g., ribbon worms) to
436 enter the nascent community. Of all treatments, the consistently cool and consistently warm
437 treatments were most different in their composition, indicating that persistent thermal stress

438 shapes not only the diversity of, but also the identity of, species within communities. Thus, the
439 higher alpha diversity and differing community structure of cool compared to warm treatments
440 may have been driven by the facilitatory ability of larger, more abundant barnacles, by more
441 and/or different species surviving under thermally benign versus thermally taxing conditions, or
442 — more likely — by a mixture of these two mechanisms. Disentangling these indirect and direct
443 effects is challenging given the experimental design employed.
444 Because foundation species (barnacle) cover was lower within the warm treatment
445 compared to the cool treatment after the first year, we anticipated that the effects of warm
446 temperatures would be magnified during the second year. However, the negative effect of
447 warming in the second summer was independent of warming in the first year. While intertidal
448 foundation species can improve the survival, growth, and diversity of associated species in the
449 face of thermal stress (Jurgens et al. 2022; Hesketh and Harley 2023), the size and density of
450 foundation species can affect their facilitative ability (Irving and Bertness 2009). Here, though *B.*
451 *glandula* had generally surpassed the size threshold for sexual maturity (~5 mm; Hines 1976),
452 they may still have been too small or sparse to effectively buffer thermal and desiccation stress
453 (Rickards and Boulding 2015) at the start of the second summer.
454 While intertidal systems are resilient up to a point, repeated atmospheric warming
455 threatens to disrupt even these historically stalwart communities (Menge et al. 2022). Our results
456 suggest that even for high-turnover barnacle bed communities (Farrell 1991), thermal stress
457 exerts lasting effects on community structure by reducing barnacle density. Increasing mean
458 temperatures and intensifying heatwaves may cause substantial mortality (Hesketh and Harley
459 2023) and accelerate shifts in ecological communities (Harris et al. 2018). Climate change also
460 encompasses multiple stressors beyond temperature that may co-occur and interact with warming

(MacLennan and Vinebrooke 2021). To understand the full risk of climate change to ecological communities, we must embrace complexity by integrating stochasticity, considering the temporal dimensions of stress, and seeking to emulate natural processes within our experimental designs.

CONFLICT OF INTEREST: The authors declare no conflicts of interest.

ACKNOWLEDGEMENTS: We thank the Coast Salish peoples on whose traditional, sovereign, and unceded territory this work was conducted. We thank S. Blain, A. Holland, and G. Brownlee for field work assistance, B. Gillespie and V. Grant for help constructing tiles, and BC Parks for site access. Thanks to R. Germain, C. Brauner, S. Dudas and two anonymous reviewers for their feedback on this work. National Geographic provided funding through AVH (EC-54154R-18). Additional support was provided to CDGH through Canadian Healthy Oceans Network (NETGP 468437-14) and an NSERC Discovery Grant (RGPIN-2016-05441).

REFERENCES

Barnes, M. 2000. The use of intertidal barnacle shells. In: Oceanography and Marine Biology: an Annual Review. Taylor & Francis, pp. 157–187.

Bates, D., Mächler, M., Bolker, B. and Walker, S. 2015. Fitting linear mixed-effects models using lme4. Journal of Statistical Software 67: 1–48.

Bjelde, B. E. and Todgham, A. E. 2013. Thermal physiology of the fingered limpet *Lottia digitalis* under emersion and immersion. Journal of Experimental Biology 216: 2858–2869.

Brooks, M.E., Kristensen, K., van Benthem, K.J., Magnusson, A., Berg, C.W., Nielsen, A., Skaug, H.J., Maechler, M. and Bolker, B.M. 2017. glmmTMB balances speed and flexibility

among packages for zero-inflated generalized linear mixed modeling. The R Journal 9: 378400

Bulleri, F., Bruno, J. F., Silliman, B. R. and Stachowicz, J. J. 2016. Facilitation and the niche: implications for coexistence, range shifts and ecosystem functioning. Functional Ecology 30: 70–78.

Dal Bello, M., Rindi, L. and Benedetti-Cecchi, L. 2019. Temporal clustering of extreme climate events drives a regime shift in rocky intertidal biofilms. Ecology 100: e02578.

Dayton, P. K. 1971. Competition, disturbance, and community organization: The provision and subsequent utilization of space in a rocky intertidal community. Ecological Monographs 41: 351–389.

Farrell, T. M. 1991. Models and mechanisms of succession: An example from a rocky intertidal community. Ecological Monographs 61: 95–113.

Fox, J. and Weisberg, S. 2019. An {R} companion to applied regression, third edition. Thousand Oaks CA: Sage.

Geller, J. B. 1991. Gastropod grazers and algal colonization on a rocky shore in northern California: the importance of the body size of grazers. Journal of Experimental Marine Biology and Ecology 150: 1–17.

Gutiérrez, J. L., Bagur, M., Lorenzo, R. A. and Palomo, M. G. 2023. A facultative mutualism between habitat-forming species enhances the resistance of rocky shore communities to heat waves. – Frontiers in Ecology and Evolution 11: 1278762.

Hamilton, H. and Gosselin, L. 2020. Ontogenetic shifts and interspecies variation in tolerance to desiccation and heat at the early benthic phase of six intertidal invertebrates. Marine Ecology Progress Series 634: 15–28.

Hammill, E. and Dart, R. 2022. Contributions of mean temperature and temperature variation to

population stability and community diversity. Ecology and Evolution 12: e8665.

Harley, C. D. G. and Lopez, J. P. 2003. The natural history, physiology, and ecological impacts of the intertidal mesopredators, *Oedoparena* spp. (Diptera, Dryomyzidae). Invertebrate Biology 122:61-73

Harley, C. D. G. 2006. Effects of physical ecosystem engineering and herbivory on intertidal community structure. Marine Ecology Progress Series 317: 29–39.

Harley, C. 2008. Tidal dynamics, topographic orientation, and temperature-mediated mass mortalities on rocky shores. Marine Ecology Progress Series 371: 37–46.

Harley, C. D. G. and O'Riley, J. L. 2011. Non-linear density-dependent effects of an intertidal ecosystem engineer. Oecologia 166: 531–541.

Harris, R. M. B., Beaumont, L. J., Vance, T. R., Tozer, C. R., Remenyi, T. A., Perkins-Kirkpatrick, S. E., Mitchell, P. J. et al. 2018. Biological responses to the press and pulse of climate trends and extreme events. Nature Climate Change 8: 579–587.

Hartig, F. 2021. DHARMa: Residual diagnostics for hierarchical (multi-level/mixed) regression models. R package version 0.4.6.

Helmuth, B., Broitman, B. R., Blanchette, C. A., Gilman, S., Halpin, P., Harley, C. D. G., O'Donnell, M. J., Hofmann, G. E., Menge, B. and Strickland, D. 2006. Mosaic patterns of thermal stress in the rocky intertidal zone: Implications for climate change. Ecological Monographs 76: 461–479.

Hersbach, H., Bell, B., Berrisford, P., Biavati, G., Horányi, A., Muñoz Sabater, J., Nicolas, J. et al. 2023. ERA5 hourly data on single levels from 1940 to present. Copernicus Climate Change Service (C3S) Climate Data Store (CDS). Accessed on 27 December 2024.

Hesketh, A. 2024. avhesketh/SVSWS: First release (v1.0.1). Zenodo.

https://doi.org/10.5281/zenodo.15054111.

Hesketh, A. 2024. The effect of single versus successive warm summers on an intertidal community [Dataset]. Zenodo. https://doi.org/10.5281/zenodo.15054128.

Hesketh, A. V. and Harley, C. D. G. 2023. Extreme heatwave drives topography-dependent patterns of mortality in a bed-forming intertidal barnacle, with implications for associated community structure. Global Change Biology 29: 165–178.

Hesketh, A. V., Schwindt, E. and Harley, C. D. G. 2021. Ecological and environmental context shape the differential effects of a facilitator in its native and invaded ranges. Ecology 102: e03478.

Hines, A. H. 1976. Reproduction in three species of intertidal barnacles from Central California. Biological Bulletin 154: 262–281.

Hughes, T. P., Kerry, J. T., Connolly, S. R., Baird, A. H., Eakin, C. M., Heron, S. F., Hoey, A. S. et al. 2019. Ecological memory modifies the cumulative impact of recurrent climate extremes. Nature Climate Change 9: 40–43.

IPCC. 2023. Climate Change 2023: Synthesis Report. Contribution of Working Groups I, II and III to the Sixth Assessment Report of the Intergovernmental Panel on Climate Change (Core Writing Team, Lee, H. and Romero, J., Eds.) IPCC, Geneva, Switzerland, pp. 35–115.

Irving, A. D. and Bertness, M. D. 2009. Trait-dependent modification of facilitation on cobble beaches. Ecology 90: 3042–3050.

Jurgens, L. J., Ashlock, L. W. and Gaylord, B. 2022. Facilitation alters climate change risk on rocky shores. Ecology 103: e03596.

Kindt, R. and Coe, R. 2005. Tree diversity analysis. A manual and software for common statistical methods for ecological and biodiversity studies. Nairobi: World Agroforestry Centre

(ICRAF).

Kordas, R. and Harley, C. 2016. Demographic responses of coexisting species to *in situ* warming. Marine Ecology Progress Series 546: 147–161.

Kordas, R. L., Dudgeon, S., Storey, S. and Harley, C. D. G. 2015. Intertidal community responses to field-based experimental warming. Oikos 124: 888–898.

Kordas, R. L., Donohue, I. and Harley, C. D. G. 2017. Herbivory enables marine communities to resist warming. Science Advances 3: e1701349.

Lee, R. H., Morgan, B., Liu, C., Fellowes, J. R. and Guénard, B. 2021. Secondary forest succession buffers extreme temperature impacts on subtropical Asian ants. Ecological Monographs 91: e01480.

Lenth, R. 2023. emmeans: Estimated marginal means, aka least-squares means. R package version 1.8.6.

Little, C. 1989. Factors governing patterns of foraging activity in littoral marine herbivorous molluscs. Journal of Molluscan Studies 55: 273–284.

Little, C., Trowbridge, C. D., Williams, G. A., Hui, T. Y., Pilling, G. M., Morritt, D. and Stirling, P. 2021. Response of intertidal barnacles to air temperature: Long-term monitoring and *in-situ* measurements. Estuarine, Coastal and Shelf Science 256: 107367.

Ma, C.-S., Wang, L., Zhang, W. and Rudolf, V. H. W. 2018. Resolving biological impacts of multiple heat waves: interaction of hot and recovery days. Oikos 127: 622–633.

MacLennan, M. M. and Vinebrooke, R. D. 2021. Exposure order effects of consecutive stressors on communities: The role of co-tolerance. Oikos 130: 2111–2121.

Menge, B. A., Gravem, S. A., Johnson, A., Robinson, J. W. and Poirson, B. N. 2022. Increasing instability of a rocky intertidal meta-ecosystem. Proceedings of the National Academy of

576 Sciences U.S.A. 119: e2114257119.
577 Montie, S. and Thomsen, M. S. 2023. Long-term community shifts driven by local extinction of
578 an iconic foundation species following an extreme marine heatwave. Ecology and Evolution
579 13: e10235.
580 Ober, G., Rognstad, R. and Gilman, S. 2019. The cost of emersion for the barnacle *Balanus*
581 *glandula*. Marine Ecology Progress Series 627: 95–107.
582 Oliver, E. C. J., Donat, M. G., Burrows, M. T., Moore, P. J., Smale, D. A., Alexander, L. V.,
583 Benthuysen, J. A. et al. 2018. Longer and more frequent marine heatwaves over the past
584 century. Nature Communications 9: 1324.
585 Oksanen, J., Blanchet, F.G., Friendly, M., Kindt, R., Legendre, P., McGlinn, D., Minchin, P.R. et
586 al. 2020. vegan: Community Ecology Package. R package version 2.6-4.
587 Pansch, C., Scotti, M., Barboza, F. R., Al-Janabi, B., Brakel, J., Briski, E., Buscholz, B. et al.
588 2018. Heat waves and their significance for a temperate benthic community: A near-natural
589 experimental approach. Global Change Biology 24: 4357–4367.
590 Perkins-Kirkpatrick, S. E. and Lewis, S. C. 2020. Increasing trends in regional heatwaves.
591 Nature Communications 11: 3357.
592 Rickards, K. and Boulding, E. 2015. Effects of temperature and humidity on activity and
593 microhabitat selection by *Littorina subrotundata*. Marine Ecology Progress Series 537: 163–
594 173.
595 Rose, N. L., Yang, H., Turner, S. D. and Simpson, G. L. 2012. An assessment of the mechanisms
596 for the transfer of lead and mercury from atmospherically contaminated organic soils to lake
597 sediments with particular reference to Scotland, UK. Geochimica et Cosmochimica Acta 82:
598 113–135.

599 Scrosati, R. A. and Ellrich, J. A. 2016. A 12-year record of intertidal barnacle recruitment in
600 Atlantic Canada (2005–2016): Relationships with sea surface temperature and phytoplankton
601 abundance. PeerJ 4: e2623–e2623.
602 Siegle, M. R., Taylor, E. B. and O'Connor, M. I. 2022. Heat wave intensity drives sublethal
603 reproductive costs in a tidepool copepod. Integrative Organismal Biology 4: obac005.
604 Silva, A. C. F., Mendonça, V., Paquete, R., Barreiras, N. and Vinagre, C. 2015. Habitat provision
605 of barnacle tests for overcrowded periwinkles. Marine Ecology 36: 530–540.
606 Stickle, W. B., Carrington, E. and Hayford, H. 2017. Seasonal changes in the thermal regime and
607 gastropod tolerance to temperature and desiccation stress in the rocky intertidal zone. Journal of
608 Experimental Marine Biology and Ecology 488: 83–91.
609 van Buuren, S., Groothuis-Oudshoorn K. 2011. mice: Multivariate Imputation by Chained
610 Equations in R. Journal of Statistical Software, 45: 1-67.
611 Vasseur, D. A., DeLong, J. P., Gilbert, B., Greig, H. S., Harley, C. D. G., McCann, K. S.,
612 Savage, V., Tunney, T. D. and O'Connor, M. I. 2014. Increased temperature variation poses a
613 greater risk to species than climate warming. Proceedings of the Royal Society B. 281:
614 20132612.
615 Vermeij, G. J. 1978. Biogeography and Adaptation: Patterns of Marine Life. Harvard University
616 Press.
617 Wood, S. N. 2011. Fast stable restricted maximum likelihood and marginal likelihood estimation
618 of semiparametric generalized linear models. Journal of the Royal Statistical Society (B) 73: 3–
619 36.
620 Wu, R. S.-S. 1981. The effect of aggregation on breeding in the barnacle *Balanus glandula*,
621 Darwin. Canadian Journal of Zoology 59: 890–892.

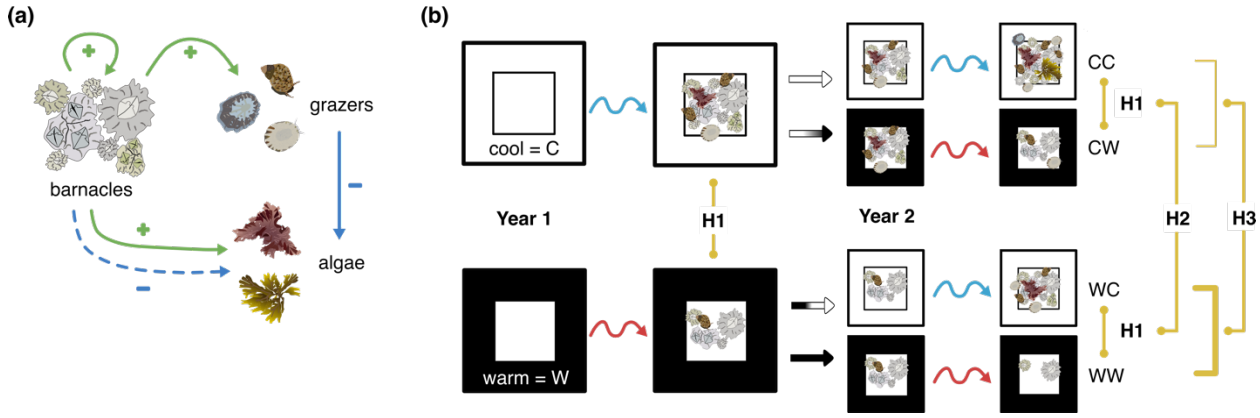
(a)
grazers
barnacles
algae
(b)
cool = C
warm = W
Year 1
H1
Year 2
CC
CW
WC
WW
H1
H1
H2
H3

Figure 1

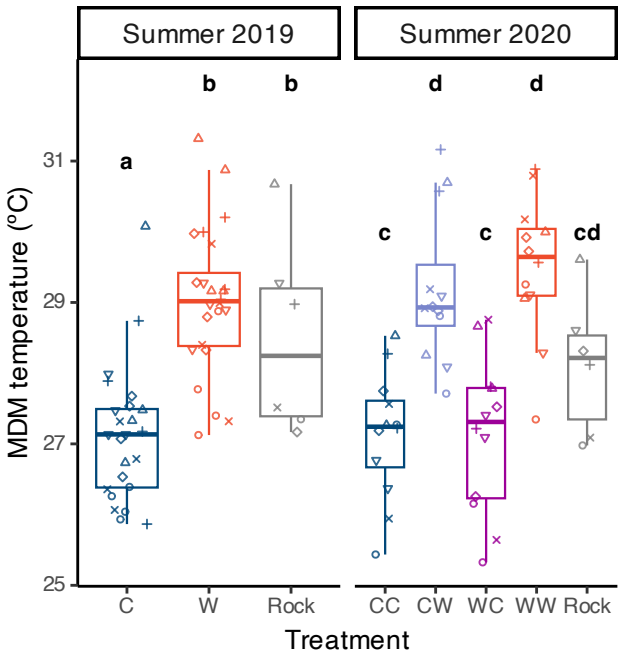

631

632 **Figure 2**

633

634

635

636

637

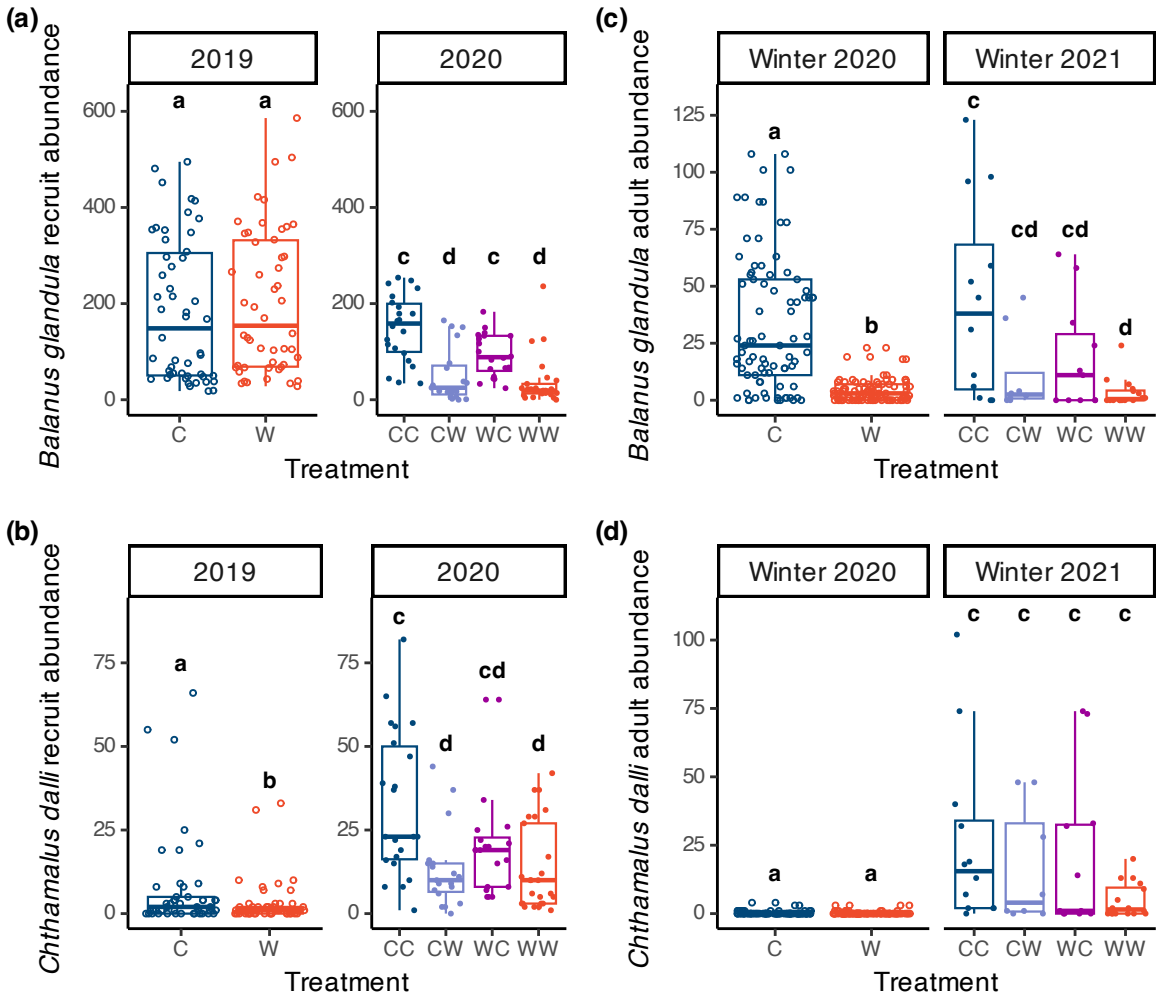
(a)
2019
2020
Balanus glandula recruit abundance
600
400
200
0
a
a
c
d
c
d
C
W
CC
CW
WC
WW
Treatment
(c)
Winter 2020
Winter 2021
Balanus glandula adult abundance
125
100
75
50
25
0
a
b
c
cd
cd
d
C
W
CC
CW
WC
WW
Treatment
(b)
2019
2020
Chthamalus dalli recruit abundance
75
50
25
0
a
b
c
d
cd
d
C
W
CC
CW
WC
WW
Treatment
(d)
Winter 2020
Winter 2021
Chthamalus dalli adult abundance
100
75
50
25
0
a
a
c
c
c
c
C
W
CC
CW
WC
WW
Treatment

Figure 3

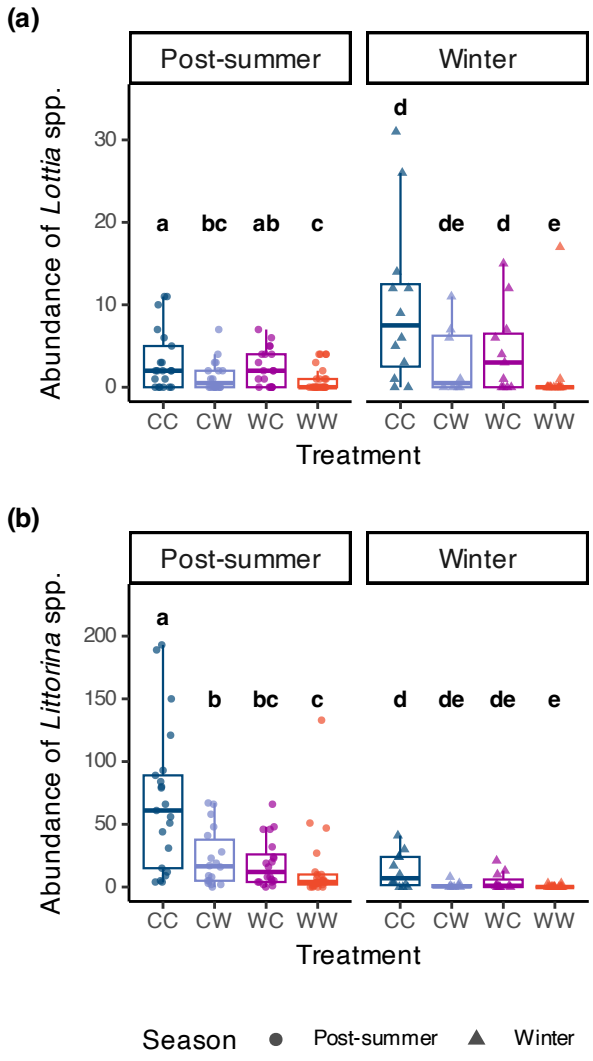
(a)
Post-summer
Winter
Abundance of Lottia spp.
30
20
10
0
a
bc
ab
c
d
de
d
e
CC
CW
WC
WW
Treatment
(b)
Abundance of Littorina spp.
200
150
100
50
0
a
b
bc
c
d
de
de
e
Season
Post-summer
Winter

Figure 4

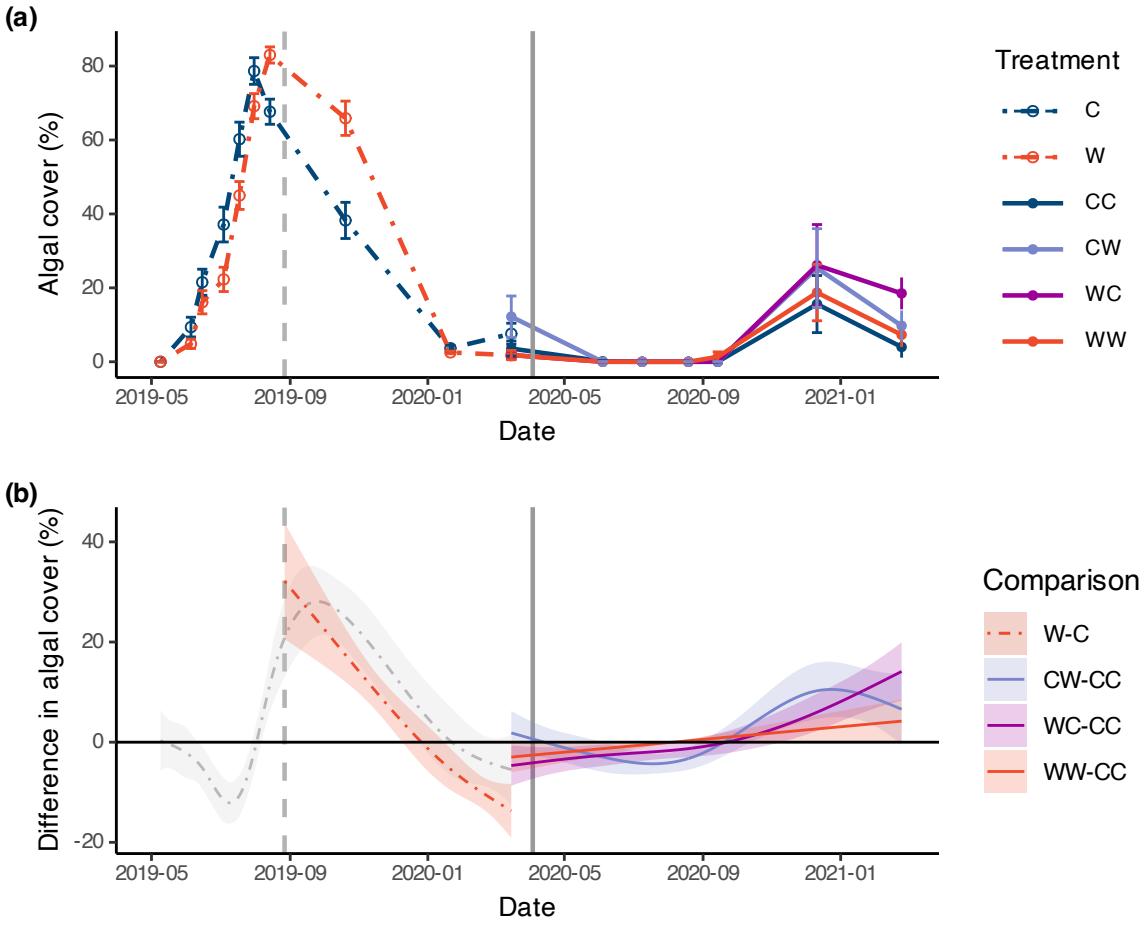
(a)
Algal cover (%)
80
60
40
20
0
2019-05
2019-09
2020-01
2020-05
2020-09
2021-01
Date
Treatment
C
W
CC
CW
WC
WW
(b)
Difference in algal cover (%)
40
20
0
-20
2019-05
2019-09
2020-01
2020-05
2020-09
2021-01
Date
Comparison
W-C
CW-CC
WC-CC
WW-CC

Figure 5

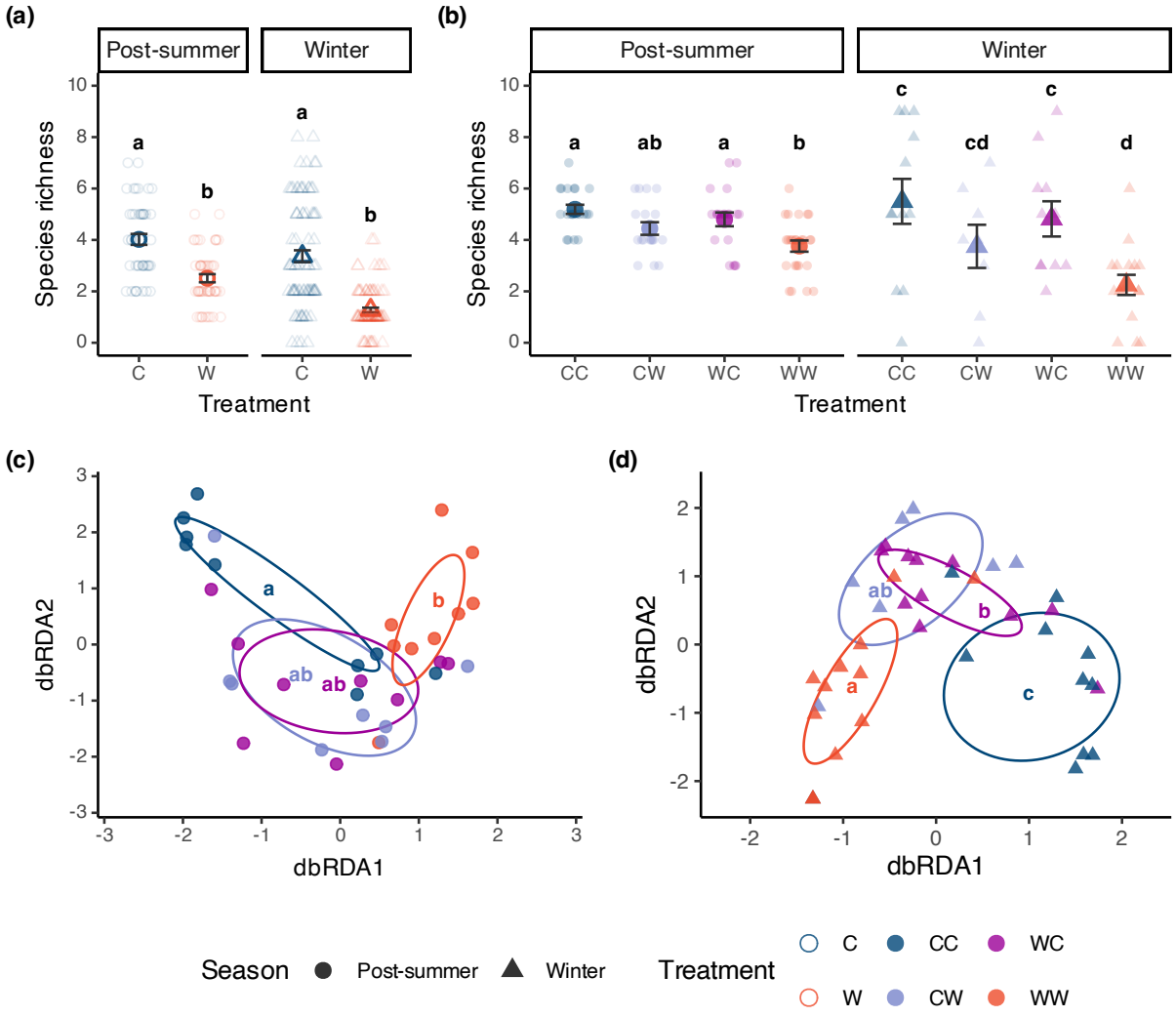

665

666 **Figure 6**

667

668

669

670

671

672

673 **Figure 1. (a)** Simplified interaction diagram for a *Balanus glandula*-dominated intertidal
674 community in the northeast Pacific. Barnacles facilitate gregarious barnacle recruitment and the
675 presence of grazers and algae through habitat provision and moisture retention, while grazers
676 consume algae. **(b)** Experimental design for this multi-year warming study and treatment
677 comparisons to address hypotheses (H1–H3). White (cool = C) tiles and black (warm = W)
678 settlement tiles were installed in the intertidal zone before the onset of summer. Tiles were then
679 exposed to summertime low tides, wherein warming was expected to drive temperature-linked
680 differences in community composition. At the start of the second year, the colour of half of each
681 treatment was swapped using heavy-duty tape, generating four treatments (CC, CW, WC, and
682 WW) that were monitored until the end of Year 2. Digital art by Amelia V. Hesketh.
683
684 **Figure 2.** Differences in residual mean daily maximum substratum temperatures of experimental
685 tiles and adjacent bedrock recorded by temperature loggers at TESNO¸EN. Points represent the
686 mean value for each experimental tile for which temperature was measured, with different shapes
687 used to represent each experimental block (n=4 per treatment per block in year one, n=2 per
688 treatment per block in year two, n=1 per block for rock temperature in both years). Only
689 temperature data collected during daytime summer low tides between 1 June – 31 August were
690 used. Bold lowercase letters represent statistically different groups, as determined by Tukey-
691 Kramer *post hoc* tests on temperature models. C = cool summer, W = warm summer, CC = cool–
692 cool, CW = cool–warm, WC = warm–cool, WW = warm–warm.
693
694 **Figure 3.** Temperature-driven differences in acorn barnacle abundance on experimental tiles at
695 TESNO¸EN, in terms of **(a)** abundance of *B. glandula* and **(b)** *C. dalli* recruits during peak

observed recruitment (*B. glandula* May 2019: n = 50; *C. dalli* June 2019: n = 46 and 50 for C and W, respectively; 4 June 2020: n = 22, 19, 20, and 25 for CC, CW, WC, and WW) and **(c)** abundance of *B. glandula* and **(d)** *C. dalli* adults at the end of the first and second winters (March 2020: n=82 for C, n=91 for W; February 2021: n = 12, 8, 11, and 16 for CC, CW, WC, and WW). Letters indicate significant differences between treatment groups determined by Type II ANOVA (year one) and Tukey-Kramer *post hoc* tests (year two). Treatment codes as in Fig. 1.

Figure 4. Temperature-driven differences in **(a)** *Lottia* spp. (limpet) and **(b)** *Littorina* spp. (littorine snail) abundance on experimental tiles at TESNO˛EN immediately following summer (September 2020; n = 21, 18, 20, and 25 for CC, CW, WC, and WW) and during winter (February 2021; n = 12, 8, 11, and 16 for CC, CW, WC, and WW). Grazers were counted on the entire 15 x 15 cm upper surface of the tiles. Bold lowercase letters indicate significant differences between treatment groups determined by Tukey-Kramer *post hoc* tests. See Fig. 1 for treatment codes.

Figure 5. (a) Temperature-driven differences in algal cover on experimental tiles at TESNO˛EN. **(b)** Pairwise differences in fitted *gamm* smoothers for algal cover in the control (C or CC) treatment and all other treatments. Shaded areas represent an approximate 95% pointwise confidence interval; when this area does not overlap zero, a significant difference can be inferred. The vertical dashed line indicates when early herbivore manipulations stopped, while the vertical solid line indicates when treatments were swapped at the beginning of year two. During year one, the grey smoother represents *gamm* smoother differences (W-C comparison) when all data are modeled; the red smoother represents *gamm* smoother differences with data

719 removed for the period that grazer manipulations were active.

720

721 **Figure 6.** Temperature-driven differences in intertidal community diversity on experimental tiles
722 at *T*ESNO¸EN. **(a)** Species richness in year one and **(b)** in year two, determined from visual
723 surveys post-summer and during late winter. Error bars represent standard error about the mean.
724 Symbols/letters denote differences between treatment groups determined by Type II ANOVA
725 (year one) and Tukey-Kramer *post hoc* tests (year two). **(c)** Community structure of destructively
726 sampled epifauna in September 2020 and **(d)** February 2021, plotted in multidimensional space
727 using distance-based redundancy analysis with Bray-Curtis distances. Each point represents a
728 single experimental tile. In year one, n = 47 and 49 for C and W, respectively post-summer and n
729 = 41 and 46 for C and W, respectively, in winter. For year two, n = 21, 18, 20, and 25 for CC,
730 CW, WC, and WW post-summer and n = 12, 8, 11, and 16 for CC, CW, WC, and WW during
731 winter. Letters denote differences between treatment groups determined using post-hoc testing
732 through *multiconstrained*.

APPENDIX S1: ADDITIONAL METHODS AND RESULTS

The effect of single versus successive warm summers on an intertidal community

Amelia V. Hesketh, Cassandra A. Konecny, Sandra M. Emry, Christopher D. G. Harley

Ecology

Tile construction

Experimental tiles consisted of a sandwich of two 15 x 15 cm squares of high-density polyethylene "puckboard" (Redwood Plastics, BC). The bottom tile (white, 9.5 mm thickness) was used to anchor the tile assembly to the underlying bedrock using two 18-8 stainless steel lag bolts (6.35 x 38.1 mm; Pacific Fasteners, BC). The lag bolts were threaded through 9.5 mm holes (with a 1.91 cm counterbore) drilled along the centre line of the bottom tile unit and screwed into plastic anchors (6.35 x 38.1 mm High-Strength Twist-Resistant Plastic Anchors for Block and Brick; McMaster-Carr, IL) set within 7.94 mm diameter holes drilled into the underlying bedrock. Four tee nuts were hammered into each of four 9.5 mm holes in the corners of the bottom tile unit, and button screws were threaded through 6.35 mm interior diameter stainless steel lock washers (Pacific Fasteners, BC) and corresponding 6.35 mm holes in the top tile units to facilitate assembly. A central 2.06 cm hole was drilled through the top tile to allow an iButton temperature logger to be installed within the experimental tile unit. To enhance epoxy adhesion while constructing the settlement area, 12–6.4 mm holes were drilled within the central 6.9 x 6.9 cm area of the top tile unit, and this area was sanded. We placed a circle of cork within the central hole before spreading a thin layer (≤ 5 mm) of Sea Goin' Poxy Putty (Permalite Plastics, Rancho Dominguez, CA) over the area. To enhance fine-scale heterogeneity of the surface, we pressed finely ground Epsom salts into the putty. Once the epoxy dried, the Epsom salts were

dissolved with tap water, leaving behind fine pock marks on the settlement surface, and the cork was removed from the central hole to create a cavity for the temperature logger. See Fig. S1 for a detailed diagram.

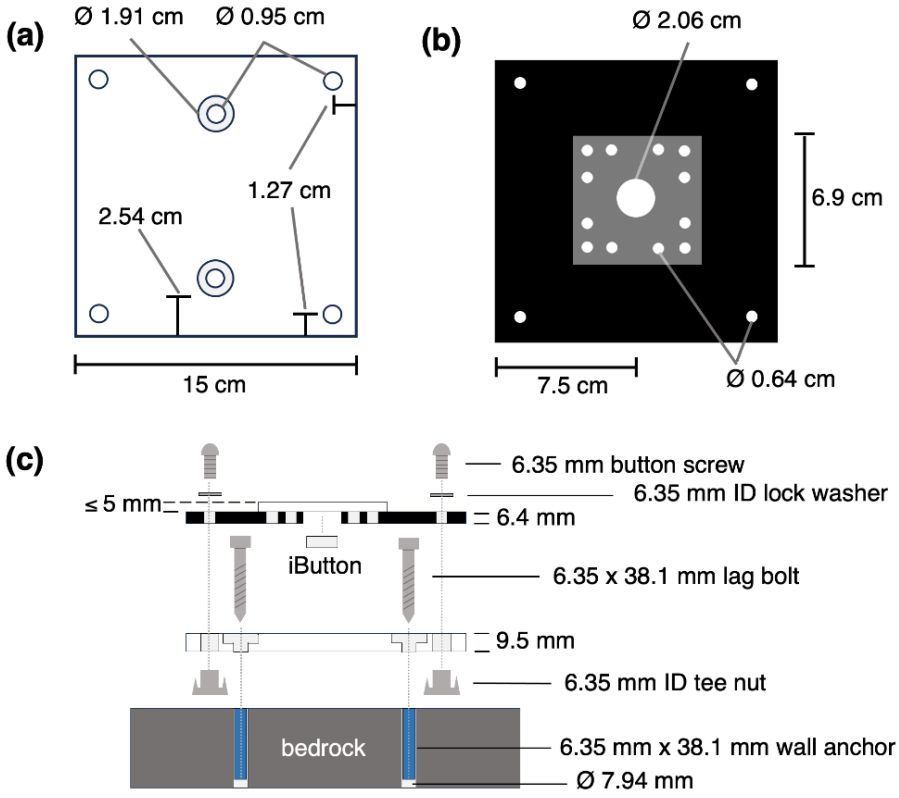

Figure S1. Diagrams of representative tile assembly used for testing the effect of artificial warming on barnacle bed communities. **(a)** Bottom unit of tile assembly, viewed from top without hardware installed. **(b)** Top unit of tile, in this case a black (warm) treatment tile, viewed from the top without hardware installed. The gray square represents the central epoxy settlement area overlying the tile. **(c)** Exploded view of tile including hardware for assembly and installation, viewed from the side. ø = diameter, ID = interior diameter. The exact position of the holes, absent the central hole for the iButton temperature logger, was not measured, so these positions have been approximated from photographs.

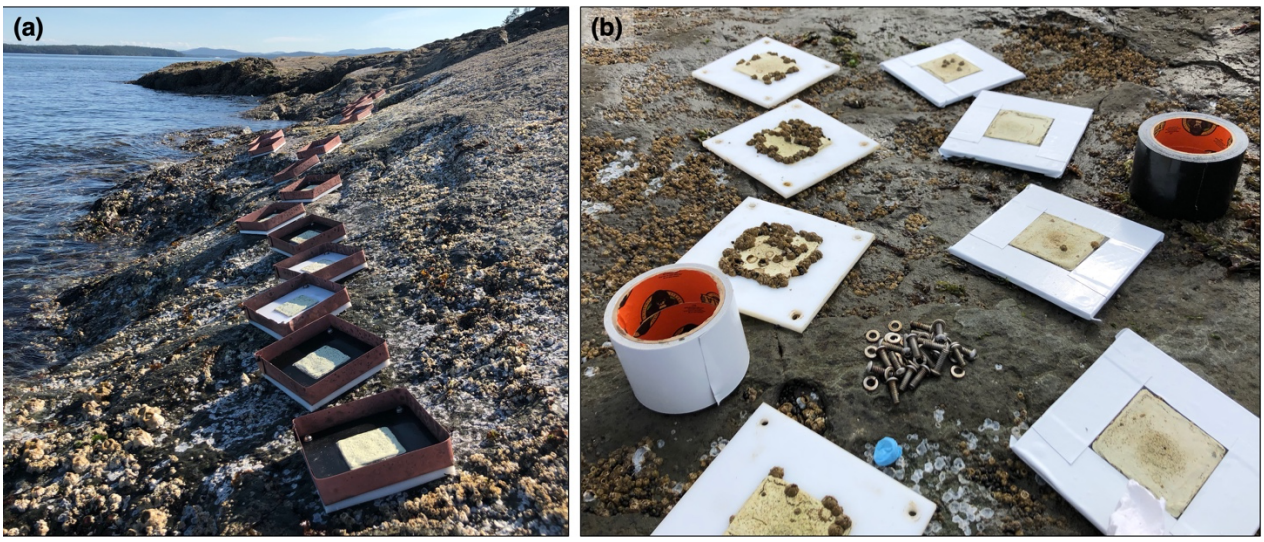

Figure S2. (a) Photograph of experimental tiles anchored in the intertidal zone at T'ESNO,EN, Salt Spring Island, still with copper fences attached to facilitate initial grazer manipulations. **(b)** Photograph of white experimental tiles without tape (cool-cool treatment; left) and white experimental tiles with tape (warm-cool treatment; right) on their upper surface, taken at the start of the second year of the experiment. Photos by Amelia V. Hesketh.

Changes to experimental design

In April 2019, we installed five blocks of 20 tiles each, half of which were white and half of which were black (N=100) at a shore level of 2.27 ± 0.06 m (mean ± SE) above Canadian chart datum. However, due to floating log disturbance within some of the blocks that were more exposed to ferry wake, several tiles were lost. In June 2019, we relocated tiles to more suitable areas to prevent log disturbance from causing further losses, arranging these same tiles within six experimental blocks of 16 tiles each, eight black and eight white (N=96; with the exception of one block, where there were nine black and seven white tiles). At this point, we added one additional white tile, as tile losses left sample sizes biased towards black tiles. All tiles were re-installed at a similar shore level of 2.34 ± 0.07 m.

We originally intended to manipulate herbivore community diversity on the experimental tiles to test how grazer diversity influences resilience to warming, an effort that was ultimately

abandoned due to the ineffectiveness of copper fences at controlling the abundance of some species, thermal stress killing others, and frequent log disturbance crushing copper inclusion fences. From May 2019 until August 2019, copper fences were affixed around each experimental tile (0.511 mm thick, 3.8 cm high above the level of the tile; Fig. S2). Ten different combinations of grazers (using *Littorina sitkana*, *Littorina scutulata*, *Lottia digitalis*, and *Lottia paradigitalis*) were established on each tile and maintained at two-week intervals from May until June 2019: all four grazers, each of the four possible limpet-littorine pairs , each grazer alone, and no grazers (n=2 per block). Despite the presence of copper fences, littorine snails — perhaps aided by wave action — were nonetheless readily able to move on and off of the tiles. We then pivoted to limpet-only treatment combinations (using both previously mentioned *Lottia* spp. and *Lottia scutum*) from June until August 2019. This manipulation employed eight limpet treatments: all three limpets, each of the three possible combinations of two limpets, each limpet alone, and no limpets. Ultimately, these treatments were also unsuccessful, as mortality in most limpet species was very high, likely due to thermal stress on the still relatively bare tiles. What limpets of these species did survive during this period were often found at the edges of tiles or wedged in the cracks between the tile and copper fence, and thus their biological function within tile communities was likely minimal. In August 2019, we thus removed the copper fences, and herbivores of all species were allowed unfettered access to tile communities thereafter.

Table S1. Design iterations employed during study of passive summertime warming on barnacle bed communities at TESNO, EN. Treatments were applied from May 2019 (two months after establishment) to the experiment endpoint in February 2021.

Design	Time period	Manipulations	Treatments	Blocks	n	Reason for change
1	8 May–5 June 2019	Temperature · herbivory (2 limpets + 2 littorines)	2 · 10 = 20	5	5	Littorine movement
2	5 June–27 August 2019	Temperature · herbivory (3 limpet spp.)	2 · 8 = 16	6	6	Log disturbance, thermal stress
3	27 August 2019–24 February 2021	Temperature year 1 · Temperature year 2	2 · 2 = 4	6	24	

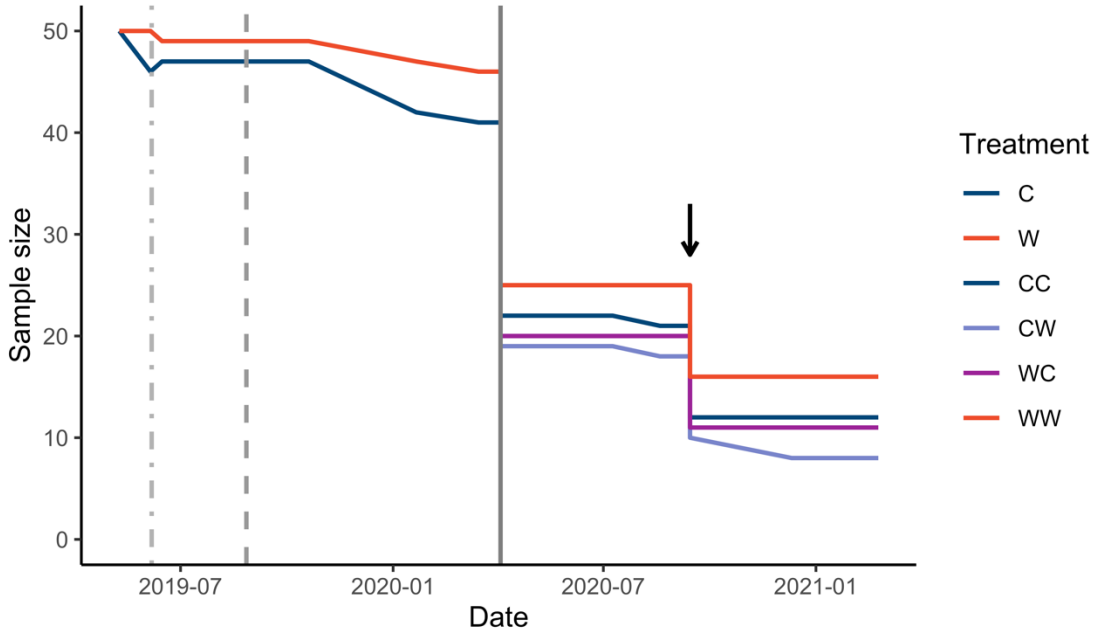

Figure S3. Changes in the number of experimental tiles within treatment groups over time. The first dashed vertical line indicates when tiles were moved in early June 2019 to avoid log damage and littorine community manipulations stopped. The second dashed line represents when grazer exclusion/inclusion fences were removed. The solid vertical line represents when year two tile treatments were established by reversing the color of half of the tiles, at which point sample sizes were effectively halved, and the arrow indicates when the first set of tiles was destructively sampled to measure epifaunal abundance and community structure in September 2020. See Fig. S2 for treatment abbreviations. CC = cool–cool, CW = cool–warm, WC = warm–cool, WW = warm–warm.

Estimating tile shore levels

Shore levels for individual tiles were estimated from temperature traces and tide data (Fisheries and Oceans Canada 2022). For each tile, temperature data from spring low tide series during the middle of summer were manually searched for three intervals where temperatures clearly transitioned from moderate sea surface temperatures one hour (typically ~12–15 ºC) to much higher aerial temperatures (>20 ºC) the next. These transitions occur when tiles become emersed after being immersed. The shore level of the tile above Canadian chart datum was approximated as the mean level of the tide between those two timepoints. These shore level values were subsequently used in filtering temperature data for plotting and analyses.

Additional temperature data

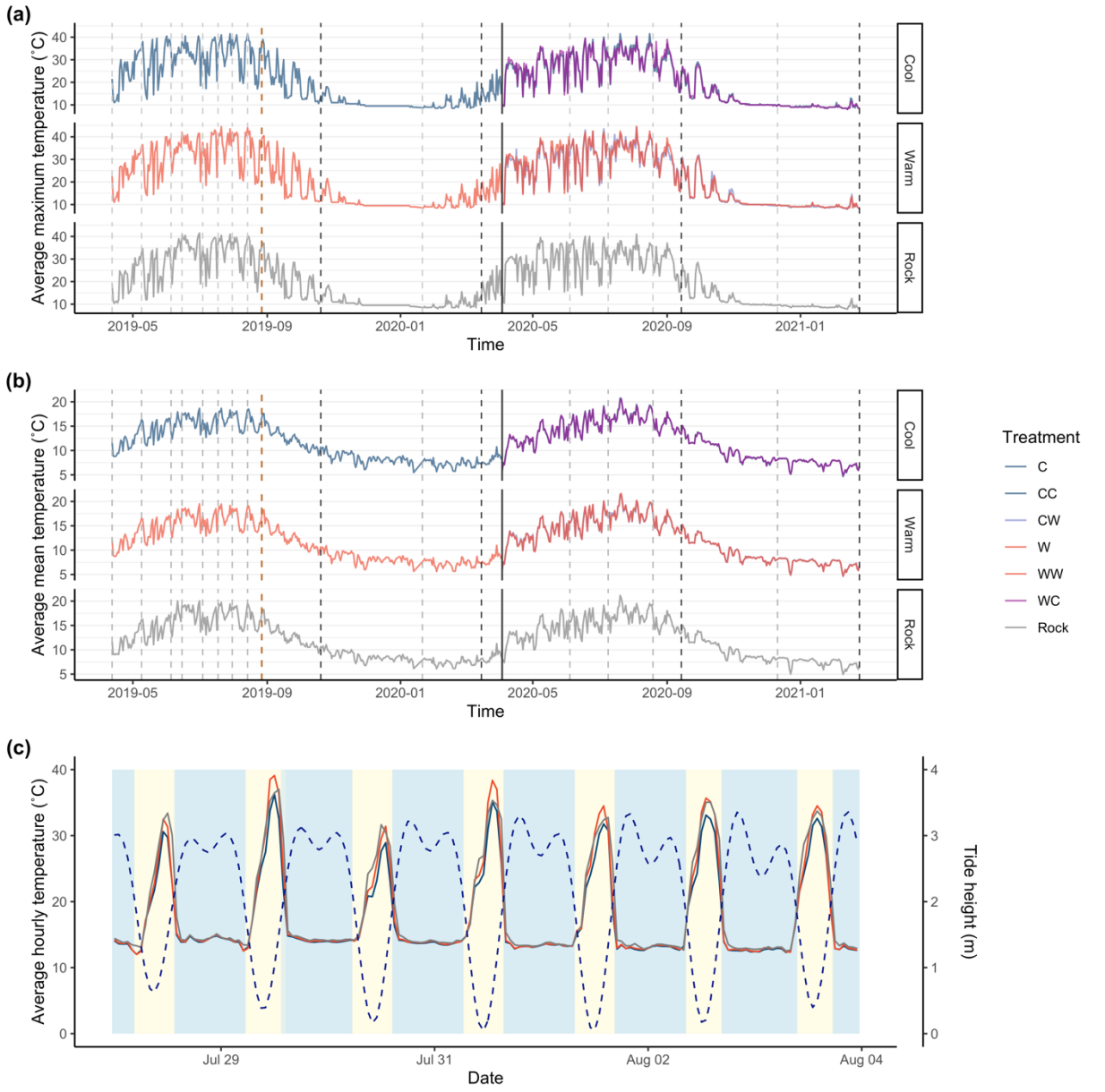

Figure S4. Temperatures of experimental tile and adjacent bedrock during a two-year passive thermal manipulation at TESNO,EN, Salt Spring Island. **(a)** Mean daily maximum and **(b)** mean temperatures over the entire experiment, averaged for each treatment. Dashed vertical lines represent when visual surveys were performed, with four darker lines representing post-summer and post-winter analysis timepoints and the single copper line representing when copper fences were removed (grazer manipulations ceased). The single solid vertical line represents the date on which treatments were swapped going into year two of the experiment. **(c)** Hourly temperatures from 28 July – 4 August 2019 averaged among all tiles in each treatment. Tide data are overlaid (height above Canadian chart datum; dashed line) to illustrate the effect of emersion (pale yellow background) and submersion (pale blue background). Treatment abbreviations as in Fig. S3.

Warm (black) tiles had higher mean temperatures than cool (white) tiles in both year one and year two (Fig. S5; ANOVA; year one: $\chi^2_2 = 37.38$, $P < 0.001$; year two: $\chi^2_4 = 78.48$, $P < 0.001$). Mean bedrock temperatures were similar to the warm treatment during the first year and all but the WW treatment during the second year (Table S10).

Table S2. Temperature conditions on experimental tiles deployed during a two-year passive thermal manipulation at TESNO, EN. Temperature data reflect only those data recorded during summertime low tides (May–August), with missing observations estimated using multiple imputation. Abbreviations as in Fig. S2. MDM = mean daily maximum, values are reported ± one standard deviation.

Period	Treatment	MDM temperature (ºC)	Mean temperature (ºC)
Year 1	C	27.1 ± 6.6	21.5 ± 4.7
	W	29.0 ± 7.4	22.6 ± 5.3
	Rock	28.5 ± 7.0	22.7 ± 5.4
Year 2	CC	27.1 ± 6.4	21.5 ± 4.8
	WC	27.1 ± 6.1	21.5 ± 4.8
	CW	29.2 ± 6.8	22.7 ± 5.2
	WW	29.5 ± 6.9	23.0 ± 5.5
	Rock	28.1 ± 6.4	22.3 ± 5.0

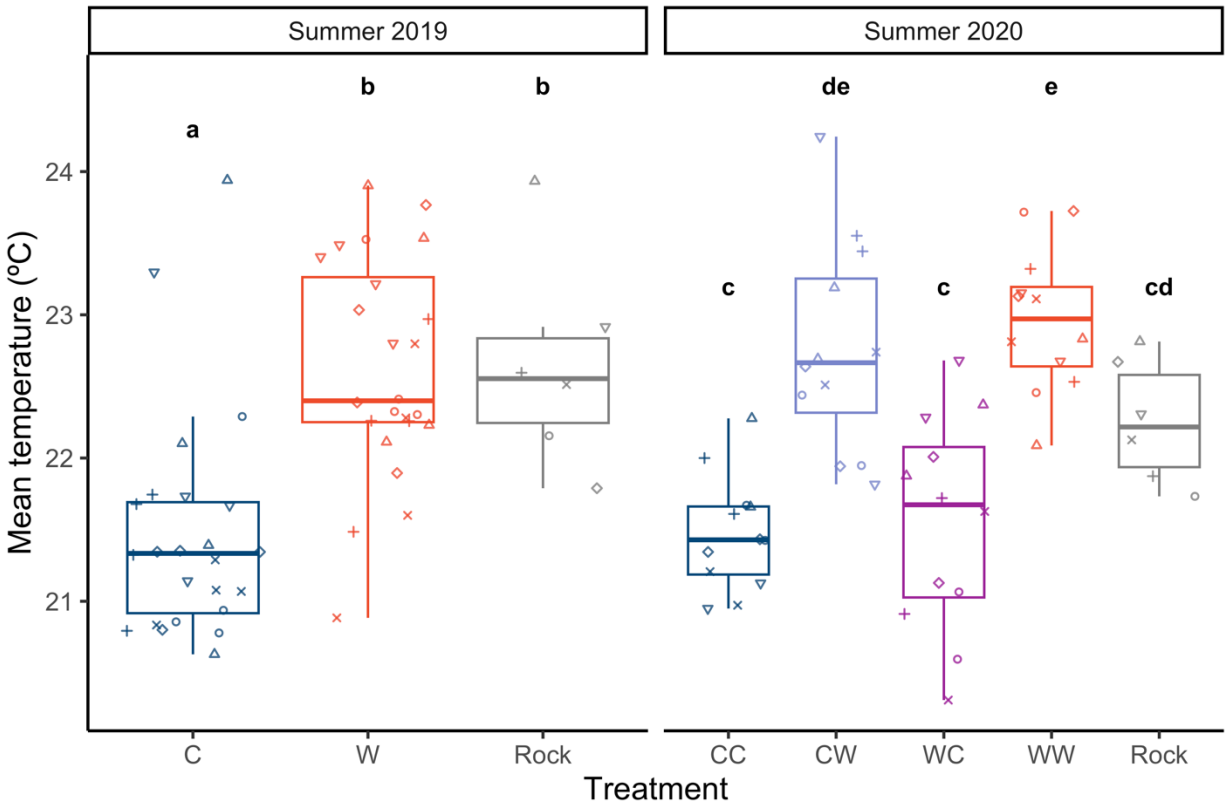

Figure S5. Differences in mean substratum temperatures during daytime summer low tides of experimental tiles and adjacent bedrock recorded by temperature loggers at TESNO, EN. Points represent the mean value for each of the six experimental blocks, using only temperatures collected during daytime summer low tides between 1 June – 31 August. In year one, n=4 per treatment per block (N=24), and in year two, n=2 per treatment per block (N=12). In both years, n = 1 for bedrock temperatures in each block. Bold letters represent treatment differences determined by Tukey *post hoc* testing. Treatment abbreviations as in Fig. S3.

Additional biological data

Table S3. Relationship between model outputs and our three initial hypotheses: H1) that warming would have a contemporaneous negative effect on the abundance and diversity of organisms; H2) that warming would have a persistent negative effect across years; and H3) that warming in year two would be magnified by (positively interact with) prior warming in year one. Here, no support is indicated by the absence of text, while the direction of the effect is communicated through colored shading (grey = no effect, blue = negative effect; orange = positive effect). Darker colors indicate a substantial directional effect, while lighter colors indicate an equivocal directional effect (*i.e.,* only at certain times of year, through *post hoc* tests). NA indicates where no model was created.

Biological response	**H1**		**H2**	**H3**
	Year 1	Year 2	Year 2	Year 2
B. glandula recruitment		Support	Support	
C. dalli recruitment	Support	Support	Support	
B. glandula adult abundance	Support	Mixed support	Mixed support	
B. glandula mortality	Support	Support		
B. glandula size	Support	Support		
C. dalli adult abundance				
Lottia spp. abundance	NA	Mixed support		
Littorina spp. abundance	NA	Support	Mixed support	
Algal cover	Support	Support		
Species richness	Support	Mixed support		
Shannon diversity (invertebrate)			Mixed support	
Shannon diversity (algae)	Support			
Community structure	NA	Mixed support	Mixed support	Mixed support
Beta diversity	NA			
Epifaunal richness	NA		Mixed support	
Epifaunal Shannon diversity	NA	Mixed support	Mixed support	

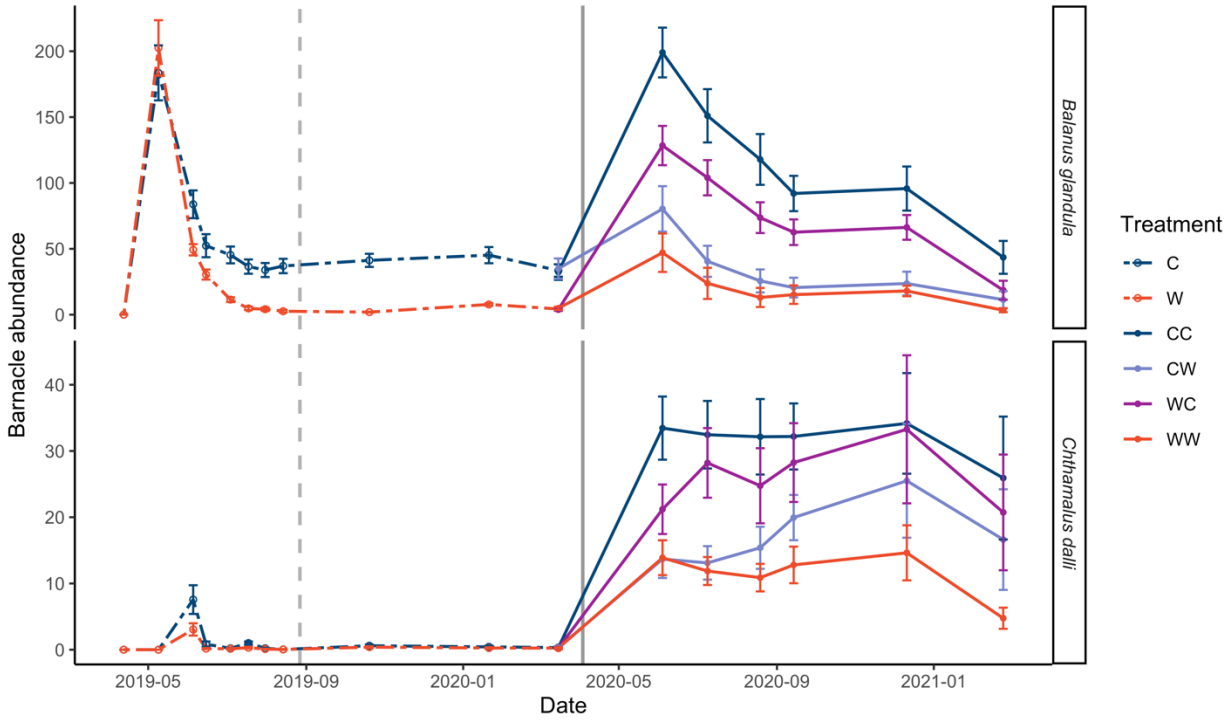

Figure S6. Mean abundance of *Balanus glandula* and *Chthamalus dalli* acorn barnacles on experimental tiles at TESNO, EN, including recruits, over the course of the entire experiment. Error bars represent standard errors about the mean. The dotted line represents the time at which experimental treats were switched from those of Year 1 to Year 2. Note that y axes are on different scales. Treatment abbreviations as in Fig. S3.

Summer mortality of *B. glandula* within each temperature treatment was measured from photographs of experimental tiles taken at four time points throughout the study. Barnacles were classified as dead if they were missing their opercular plates but had lateral plates partly or fully intact. Proportional mortality was analyzed to complement density counts and more directly track thermally driven patterns of post-recruitment mortality. This metric was calculated by dividing the number of dead barnacles by the number of total (live + dead) barnacles on each tile (Fig. S7a). We also present the abundance of dead barnacles, the density of which may influence habitat availability for facilitated species (e.g., littorine snails; Fig S7b). Proportional mortality was multiplied by 100 to yield a percentage mortality, and this metric was modeled in the same way as barnacle size, this time using the package *glmmTMB* with a Tweedie distribution. In the

first summer, *B. glandula* mortality was substantially higher in the warm relative to the cool treatment (Type II ANOVA; $\chi^2_1 = 32.633$, $P < 0.001$). In the second summer, *B. glandula* mortality was higher where temperatures were experienced contemporaneously, but more so where conditions were previously cool and barnacles were thus more abundant (CW treatment; Type III ANOVA; $\chi^2_1 = 4.93$, $P = 0.0264$).

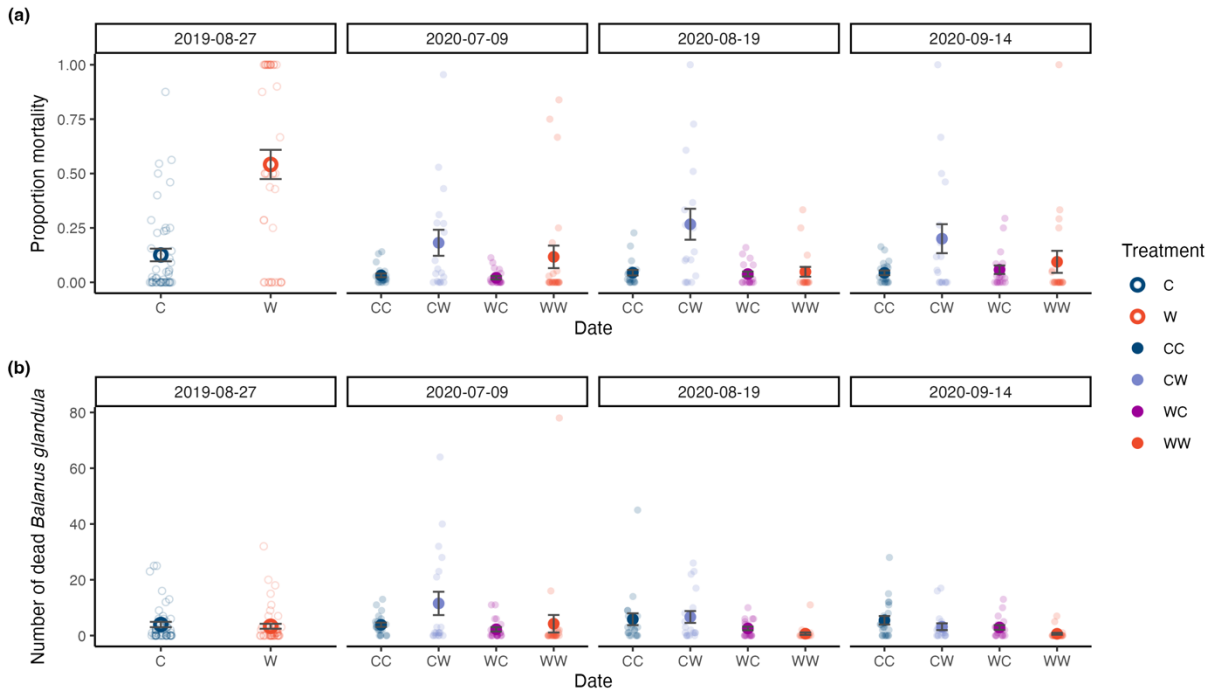

Figure S7. Summer mortality of *B. glandula* on experimental tiles at TESNO, EN at four time points during the two-year passive thermal manipulation, in terms of **(a)** proportion mortality and **(b)** number of dead individuals. Barnacles were counted as dead if valves were missing but lateral plates were fully or partially intact. Error bars about the mean indicate standard error. Sample sizes varied between timepoints and treatments and are reported in Table S4. Treatment abbreviations as in Fig. S3.

Table S4. Sample sizes associated with growth and mortality measurements for different treatments and time points.

Date	Treatment	Growth sample size	Mortality sample size
2019-08-27	C	448	47
	W	37	49
2020-07-09	CC	219	22
	CW	113	19
	WC	192	20
	WW	137	25
2020-08-19	CC		21
	CW		18
	WC		20
	WW		25
2020-09-14	CC	196	21
	CW	98	18
	WC	160	20
	WW	112	25
2020-12-11	CC	120	
	CW	58	
	WC	86	
	WW	90	

The size of *Balanus glandula* individuals were measured from photographs taken at four timepoints during the study to determine the effect of cool and warm temperatures the size of barnacles within a cohort. In each photograph, ten barnacle individuals were haphazardly selected, and the basal diameter (in mm) of these individuals was measured (Fig. S8). Log-transformed sizes were modeled in relation to treatment (in year one) or a multiplicative combination of treatments in year one and year two and sampling date (in year two). A random intercept effect of block (in year one) or of individual tile nested within experimental block (in year two) was included to account for repeated measures in space and time. Models were

constructed using the *lmer* function in the *lme4* package and assumptions checked using the *DHARMa* package. Models did not suffer from temporal autocorrelation. Models were tested via *Anova* through the *car* package, either a Type II test if no interaction was present (year one) or a Type III Wald F test with Kenward-Roger degrees of freedom (year two). In the first year, *B. glandula* within the cool treatment were substantially larger than those in the warm treatment (Type II ANOVA; $F_{1, 483} = 49.20$, $P < 0.001$). In the second year, the WW treatment generally hosted smaller barnacles than the other three treatments, indicating a negative interactive effect of warm temperatures in the first and second summer on barnacle size. However, the strength of this interaction varied across sampling dates (Type III ANOVA; $F_{2,1552} = 6.92$, $P = 0.00102$), possibly because the negative effect of warm temperatures in year one tended to wane over time.

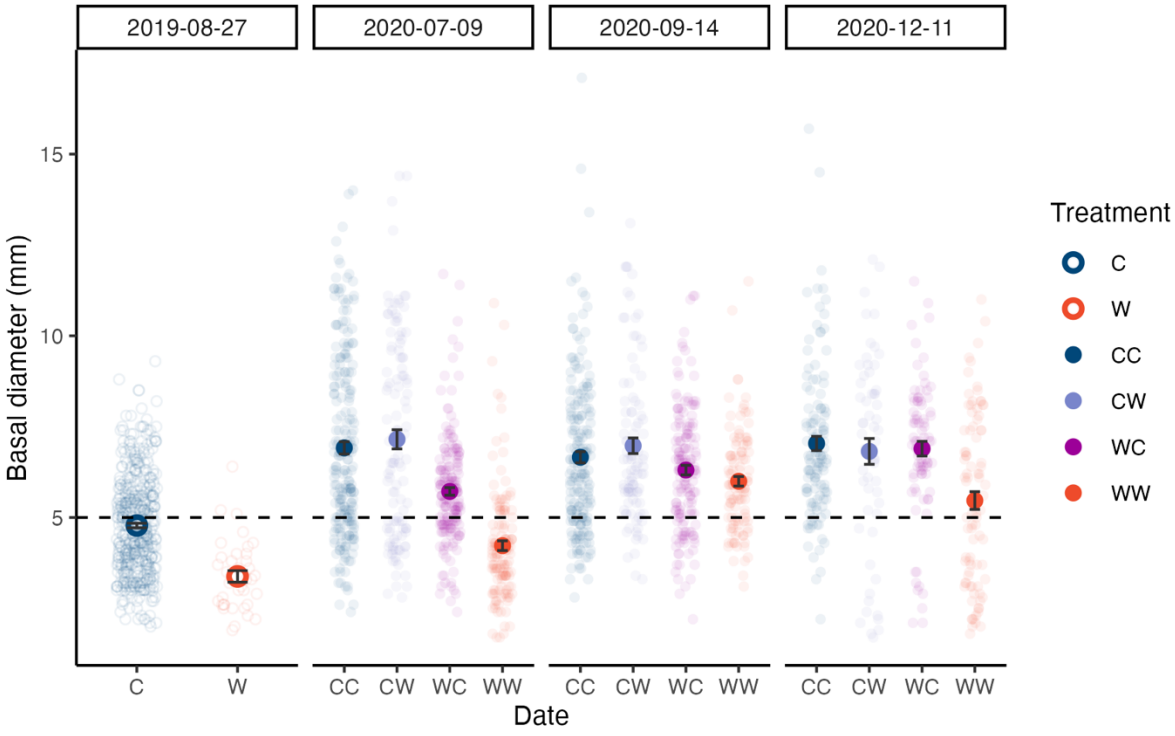

Figure S8. Basal diameter of *Balanus glandula* on experimental tiles at TESNO, EN at four time points during the two-year passive thermal manipulation. The dashed horizontal line represents the typical size of this species at sexual maturity (Hines 1978). Error bars about the mean indicate standard error. Sample sizes varied between timepoints and treatments and are reported in Table S3. Treatment abbreviations as in Fig. S3.

Here, we present the abundance of common gastropod grazers (*Lottia* spp. and *Littorina* spp.) present on experimental tiles over the second year of the study (Fig. S9). Grazers present on the entire face of each tile were included in these counts. Differences in grazer abundance were analyzed at key timepoints (immediately after summer thermal stress and after winter recovery); these results are presented in the main text.

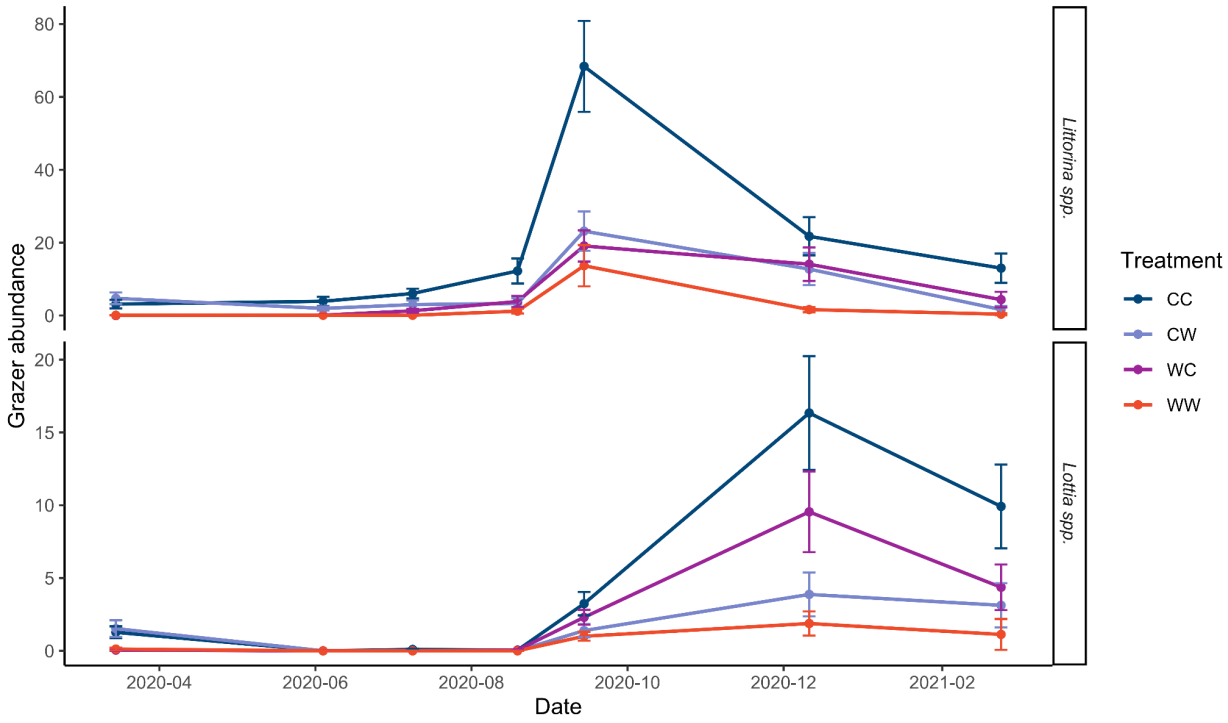

Figure S9. Mean abundance of *Lottia* spp. and *Littorina spp.* gastropod grazers on experimental tiles at TESNO, EN, including recruits, over the course of the entire experiment. Error bars represent standard errors about the mean. Note that y axes are on different scales. Treatment abbreviations as in Fig. S3.

Temporal patterns in invertebrate Shannon diversity mirrored patterns in overall species richness; diversity remained low in the first year, exhibited a peak in fall of the second year, and gradually declined thereafter (Fig. S10a–b). In the first year, the negative effect of warm temperatures on Shannon diversity was apparent in late winter (Fig. S11a; Type II ANOVA; $\chi^2_1 = 26.67$, $P < 0.001$), but not at the end of summer. In the second year, post-summer invertebrate

Shannon diversity was significantly reduced by warm temperatures during the first summer (Type III ANOVA; $\chi^2_1 = 7.35$, $P = 0.00669$). Tukey-Kramer *post hoc* tests showed that the successively warm treatment (WW) had substantially lower algal cover than the successively cool treatment (CC) and the warm–cool treatment (WC), but not the cool–warm treatment (CW). During the winter, a marginally insignificant effect of warm temperatures applied during the first year remained (Type III ANOVA; $\chi^2_1 = 3.52$, $P = 0.0605$), and *post hoc* comparisons demonstrated that the only substantial treatment difference was been the consistently cool and consistently warm treatments (*emmeans*; t ratio = 3.62, df = 41, $P = 0.0042$).

Algal Shannon diversity was highest in winter, mostly because cover became low and sometimes nonexistent from late summer to early fall (Figs. S10c). However, algal Shannon diversity was relatively unaffected by temperature treatment (Fig. S11c). Where temperatures were cooler during the first year of the experiment, algal diversity was higher (Type II ANOVA; $\chi^2 = 9.48$, $P = 0.00208$). In the second year of the experiment, algal cover was highly variable within treatment groups at the end of the winter, and Shannon diversity was similar among treatments.

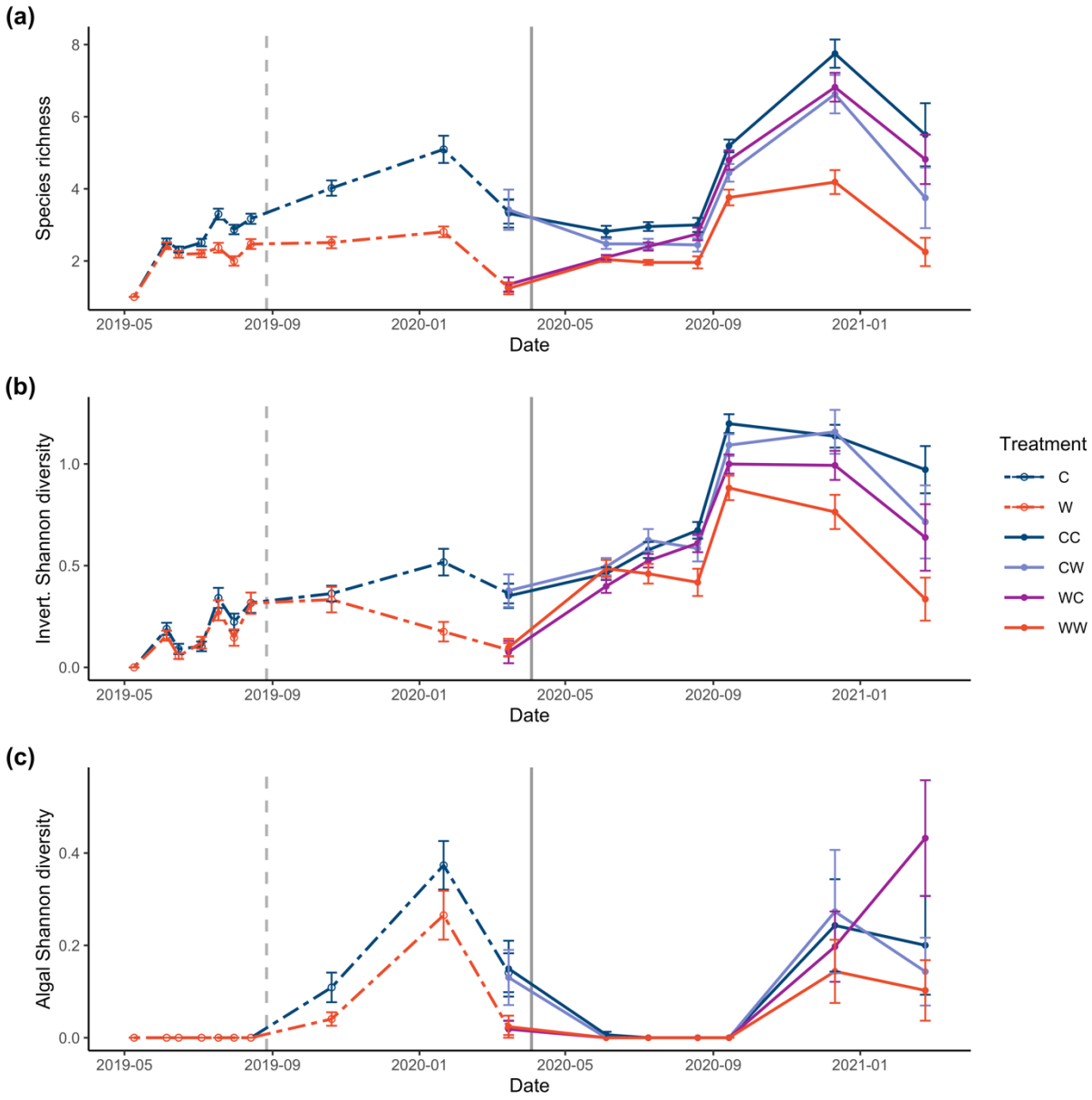

Figure S10. The effect of temperature treatments on alpha diversity of experimental communities over time, as described by changes in the **(a)** species richness of whole tile communities and Shannon diversity of **(b)** the invertebrate community and **(c)** the algal community. Error bars represent standard errors about the mean. The dotted vertical line represents the time at which experimental treatments were switched from those of Year 1 to Year 2. Note that y axes are on different scales. Treatment abbreviations as in Fig. S3.

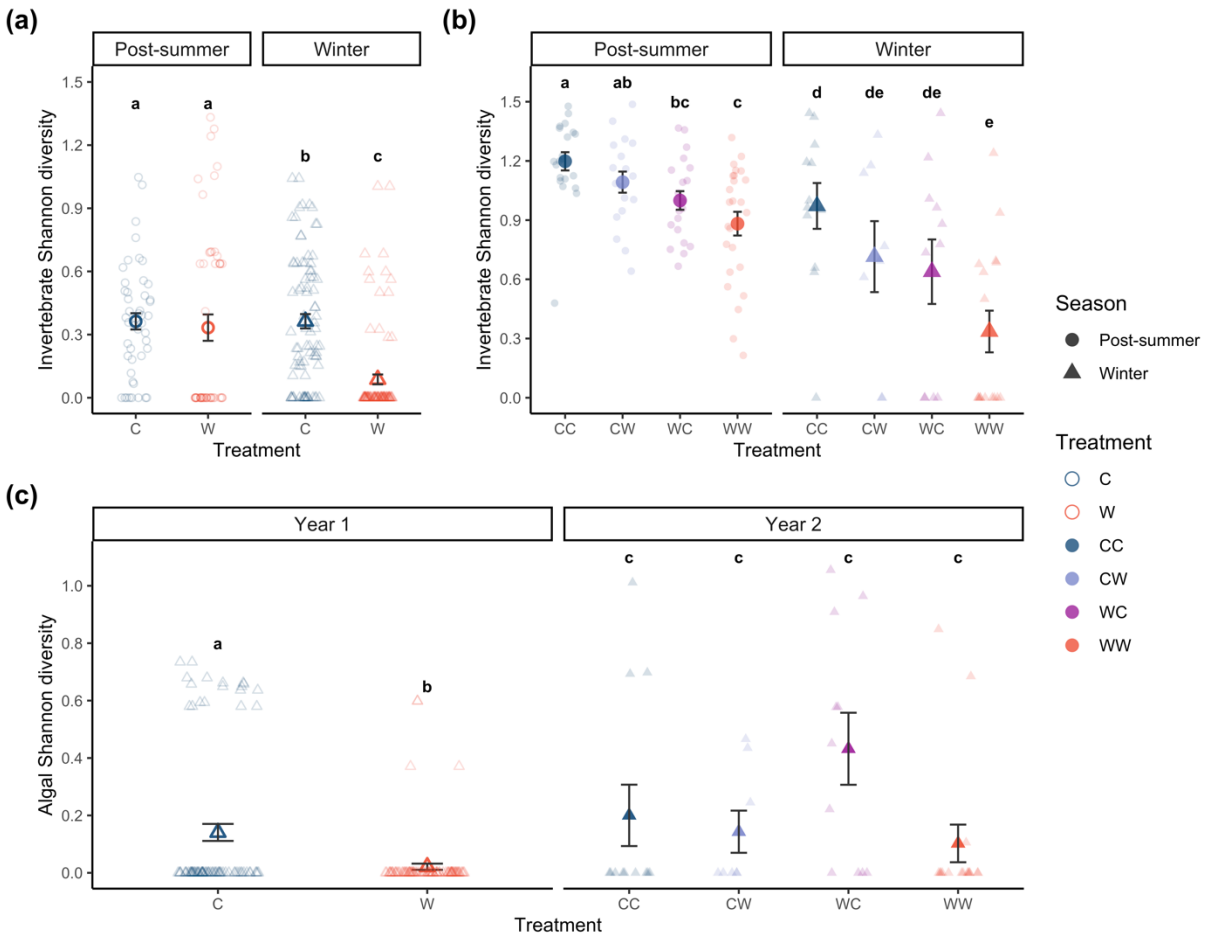

Figure S11. Shannon diversity of the **(a)** invertebrate community during the first year, **(b)** invertebrate community during the second year, and **(c)** algal community during the entire two-year passive warming experiment at TESNO, EN. Samples were obtained through visual surveys. Error bars represent standard error about the mean. Differences between treatment groups, as determined using Tukey-Kramer *post hoc* tests, are indicated through brackets (ns = non-significant) or lowercase letters. Treatment abbreviations as in Fig. S3.

The richness and Shannon diversity of destructively sampled tile epifaunal communities were also examined (Fig. S12; Table S5). Richness was similar between sampling timepoints, and was not particularly affected by warm temperatures (Fig. S12a). In September 2020, *post hoc* comparisons demonstrated a significant difference between the consistently cool and consistently warm treatment (z ratio = 3.08, $P = 0.0112$; Appendix S2: Table S56). In February 2021, warm temperatures in both the first year and second year had marginally insignificant

effects on reducing species richness (Type III ANOVA; treatment_{y1}: $\chi^2_1 = 3.64$, $P = 0.0565$; treatment_{y2}: $\chi^2_1 = 3.55$, $P = 0.0595$). Pairwise comparisons demonstrated that the CC and WC treatments had higher richness than the WW treatment (Appendix S2: Table S58). Trends in Shannon diversity were similar (Fig. S12b); temperature treatments drove no overall effects on diversity, but *post hoc* comparisons showed that the WW treatment was significantly lower in its diversity than other treatments at both timepoints (Appendix S2: Tables S60, S62).

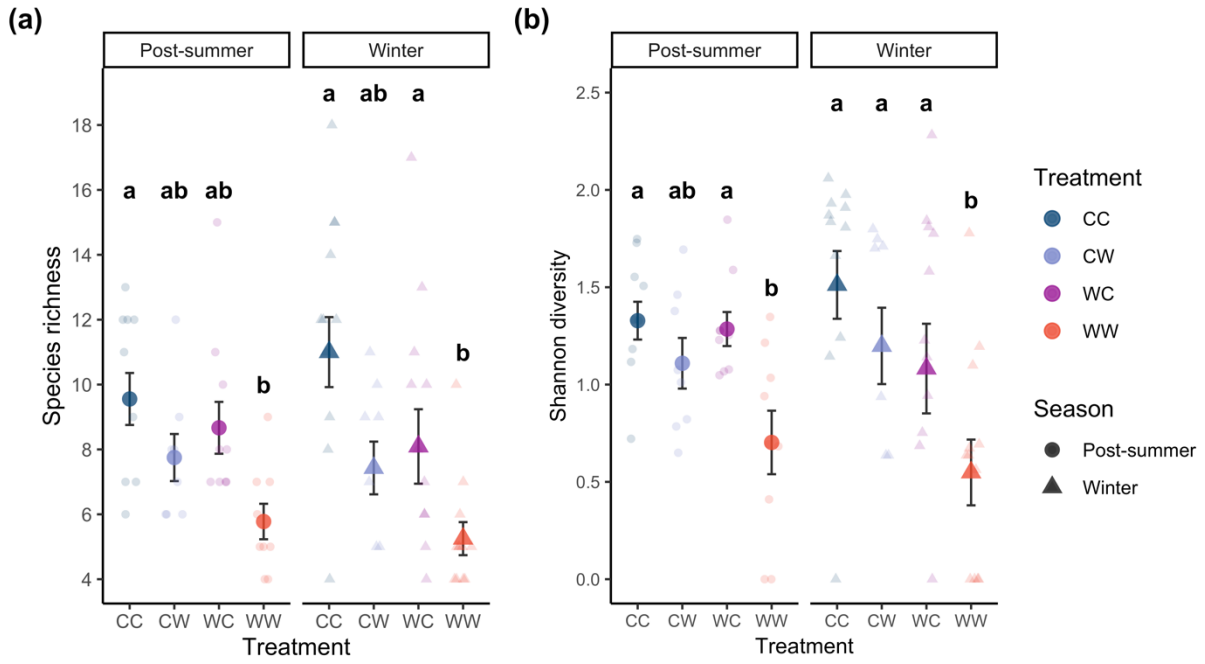

Figure S12. (a) Species richness and **(b)** Shannon diversity of epifaunal community within destructively sampled experimental tiles in the second year of a multi-year passive warming experiment at TESNO, EN. Error bars represent standard error about the mean. Differences between treatment groups, as determined using Tukey-Kramer *post hoc* tests, are indicated using lowercase letters. Treatment abbreviations as in Fig. S3.

Table S5. Inventory of epifaunal taxa found during destructive surveys of intertidal barnacle bed communities on experimental tiles at TESNO, EN.

Taxon name	Authority
Amphipoda	Latreille, 1816
Anthopleura elegantissima	Brandt, 1835
Annelida	
Arachnida	
Cyprid larva	Burmeister, 1834
Copepoda	Milne Edwards, 1840
Dynamenella sheareri	Hatch, 1947
Emplectonema gracile	Johnston, 1837
Hymenoptera	
Insecta	
Isopoda	Latreille, 1817
Lasaea rubra	Montagu, 1803
Littorina scutulata	Gould, 1849
Littorina sitkana	Philippi, 1846
Lottia digitalis	Rathke, 1833
Lottia paradigitalis	Fritchman, 1960
Lottia pelta	Rathke, 1833
Lottia scutum	Rathke, 1833
Lottia sp.	Gray, 1833
Mytilus sp.	Linnaeus, 1758
Neostylidium eschrichtii	Middendorff, 1849
Nemertea	
Oedoparena sp.	Curran, 1934
Onchidoris bilamellata	Linnaeus, 1767
Pagurus hirsutiusculus	Dana, 1851
Platyhelminthes	Minot, 1876
Polychaeta	Grube, 1850
Polychaeta	Grube, 1850
Sabellidae	Latreille, 1825
Syllidae	Grube, 1850
Telmatogeton sp.	Schiner 1866

Changes in community structure were plotted through time to examine qualitative patterns of change through community trajectory analysis in the *ecotraj* package (version 0.0.1; De Cáceres et al. 2019). To do this, the 'average' community structure of each treatment group at each timepoint, using abundance and cover data from visual surveys, was determined by averaging species abundance or cover for all experimental tiles in each treatment, and distance-based redundancy analysis was performed on these averaged communities for all timepoints with 999 random starts and autotransformation of data using Bray-Curtis distances.

Differences in the temperature of tile treatments drove divergences in the biological community inhabiting these tiles over time (Fig. S13). Cool and warm treatments quickly diverged in composition over the first summer, and this divergence grew through the winter. Communities followed a similar trajectory during the first part of the second summer. However, treatment differences were apparent by the end of the summer, with CC and WC treatments grouping together and WW and CW treatments grouping together. Following the second winter, the WW and CC treatments were quite similar in composition to the warm and cool treatments, respectively, at the same time the previous year, while the CW and WC treatments were intermediate in their composition.

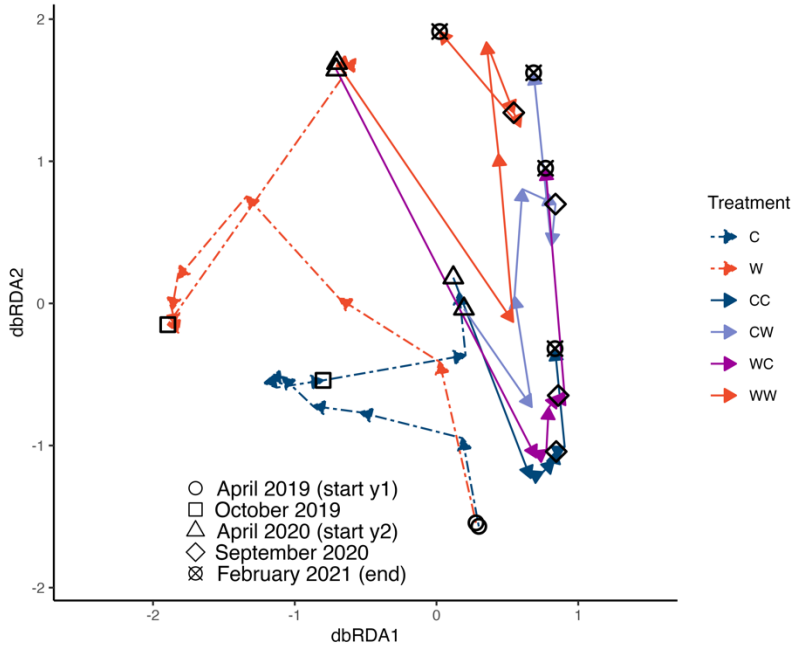

Figure S13. Trajectory plot for experimental tile communities over the course of the experiment from April 2019 to February 2021. Trajectories represent the 'average' community — calculated by averaging the abundance of each species across experimental tile units in each treatment at each timepoint — with the start and end terminus of each arrow based on Bray-Curtis dissimilarities among communities. The direction of arrows shows the flow of time from the beginning to the end of the experiment, and the length of each arrow correlates with the magnitude of community shift between timepoints. Different points along each treatment trajectory help visually identify key timepoints during the experiment (experiment start, end of summer in y1=year one, start of y2=year two, end of summer in y2, experiment end). Sample sizes for each treatment group changes through time. See Fig. S3 for treatment abbreviations.

REFERENCES

De Cáceres, M., Coll, L., Legendre, P., Allen, R., Wiser, S., Fortin, M., Condit, R., and Hubbell, S. 2019. Trajectory analysis in community ecology. Ecological Monographs **89**: e01350.

Fisheries and Oceans Canada. 2022. Tides, currents, and water levels. https://tides.gc.ca/en.

Hines, A.H. 1978. Reproduction in three species of intertidal barnacles from Central California. The Biological Bulletin 154: 262–281.

APPENDIX S2: STATISTICAL OUTPUTS

The effect of single versus successive warm summers on an intertidal community

Amelia V. Hesketh, Cassandra A. Konecny, Sandra M. Emry, Christopher D. G. Harley

Ecology

Analysis 1: Substratum temperature

Model S1

Mean daily maximum temperature ~ treatment + (1 | tile) + (1 | date) + ar1(date – 1 | tile)
Error distribution: Gaussian

Table S1. Model summary table for Model S1, an autoregressive linear mixed effects model testing the effect of treatment on mean daily maximum temperature recorded by temperature loggers during daytime summer low tides of the first year of the thermal manipulation. Random intercept effects were included for individual tile and sampling date, with an autoregressive order 1 process for sampling date to reduce temporal autocorrelation. Coefficients given are relative to the cool treatment, and the model was tested using a Type II ANOVA. SE = standard error, df = degrees freedom.

Term	Coefficient	SE	χ^2	df	*P*
Intercept	27.038	0.634			
Treatment–Rock	1.410	0.477	40.53	2	**1.59×10^{-9}**
Treatment–Warm	1.896	0.302			

Table S2. Tukey-Kramer *post hoc* comparison of the mean daily maximum temperatures within treatment groups in year one of the thermal manipulation. SE = standard error, C = cool treatment, W = warm treatment

Contrast	Estimate	SE	df	*t* ratio	*P*
C–Rock	-1.410	0.477	6575	-2.955	**0.0088**
C–W	-1.896	0.302	6575	-6.284	**<0.0001**
Rock–W	-0.486	0.477	6575	-1.020	0.564

Table S3. Model summary table for Model S1, an autoregressive linear mixed effects model testing the effect of treatment on mean daily maximum temperature recorded by temperature loggers during daytime summer low tides of the second year of the thermal manipulation. Random intercept effects were included for individual tile and sampling date, with an autoregressive order 1 process for sampling date to reduce temporal autocorrelation. Coefficients given are relative to the cool summer – cool summer (CC) treatment, and the model was tested using a Type II ANOVA. SE = standard error, df = degrees freedom. CW = cool summer – warm summer, WC = warm summer – warm summer, WW = warm summer – warm summer.

Term	Coefficient	SE	χ^2	df	*P*
Intercept	27.092	0.634			
Treatment–CW	1.960	0.425			
Treatment–Rock	1.034	0.521	52.34	4	**1.17×10^{-10}**
Treatment–WC	-0.010	0.425			
Treatment–WW	2.345	0.425			

Table S4 Tukey-Kramer *post hoc* comparison of the mean daily maximum temperature of treatment groups in year two of the thermal manipulation. See Table S3 for treatment codes and abbreviations.

Contrast	Estimate	SE	df	*t* ratio	*P*
CC–CW	-1.960	0.425	6580	-4.61	**<0.0001**
CC–Rock	-1.034	0.521	6580	-1.99	0.273
CC-WC	0.010	0.425	6580	0.024	1.00
CC–WW	-2.345	0.425	6580	-5.52	**<0.0001**
CW–Rock	0.927	0.521	6580	1.78	0.386
CW–WC	1.970	0.425	6580	4.63	**<0.0001**
CW–WW	-0.385	0.425	6580	-0.91	0.895
Rock–WC	1.044	0.521	6580	2.01	0.264
Rock–WW	-1.311	0.521	6580	-2.52	0.0866
WC–WW	-2.355	0.425	6580	-5.54	**<0.0001**

Model S2

Mean daily temperature ~ treatment + (1 | tile) + (1 | date) + ar1(date – 1 | tile)
Error distribution: Gaussian

Table S5. Model summary table for Model S2, an autoregressive linear mixed effects model testing the effect of treatment on daily mean temperatures recorded by temperature loggers during daytime summer low tides of the first year of the thermal manipulation. Random intercept effects were included for individual tile and sampling date, with an autoregressive order 1 process for sampling date to reduce temporal autocorrelation. Coefficients given are relative to the cool treatment, and the model was tested using a Type II ANOVA. df = degrees of freedom, SE = standard error.

Term	Coefficient	SE	χ^2	df	*P*
Intercept	21.415	0.452			
Treatment–Rock	1.192	0.318	37.38	2	**7.62×10^{-9}**
Treatment–Warm	1.158	0.201			

Table S6. Tukey-Kramer *post hoc* comparison of the mean daily temperature of treatment groups in year one of the thermal manipulation. SE = standard error, C = cool treatment, W = warm treatment

Contrast	Estimate	SE	df	*z* ratio	*P*
C–Rock	-1.192	0.317	6575	-3.75	**0.0005**
C–W	-1.158	0.201	6575	-5.77	**<0.0001**
Rock–W	0.034	0.317	6575	0.11	0.994

Table S7. Model summary table for Model S2, an autoregressive linear mixed effects model testing the effect of treatment on mean daily temperature recorded by temperature loggers during daytime summer low tides of the second year of the thermal manipulation. Random intercept effects were included for individual tile and sampling date, with an autoregressive order 1 process for sampling date to reduce temporal autocorrelation. Coefficients given are relative to the cool summer – cool summer (CC) treatment, and the model was tested using a Type II ANOVA. See Table S3 for abbreviations.

Term	Coefficient	SE	χ^2	df	*P*
Intercept	21.449	0.465	78.48	4	**3.66×10^{-16}**
Treatment–CW	1.212	0.211			
Treatment–Rock	0.806	0.258			
Treatment–WC	0.063	0.211			
Treatment–WW	1.463	0.211			

Table S8. Tukey-Kramer *post hoc* comparison of mean daily temperature of treatment groups in year two of the thermal manipulation. See Table S3 for treatment codes and abbreviations.

Contrast	Estimate	SE	df	*z* ratio	*P*
CC–CW	-1.212	0.211	6580	-5.75	**<0.0001**
CC–Rock	-0.806	0.258	6580	-3.12	**0.0155**
CC-WC	-0.063	0.211	6580	-0.298	0.998
CC–WW	-1.463	0.211	6580	-6.94	**<0.0001**
CW–Rock	0.406	0.258	6580	1.57	0.516
CW–WC	1.150	0.211	6580	5.45	**<0.0001**
CW–WW	-0.251	0.211	6580	-1.19	0.759
Rock–WC	0.744	0.258	6580	2.88	**0.0326**
Rock–WW	-0.656	0.258	6580	-2.54	0.0819
WC–WW	-1.400	0.211	6580	-6.64	**<0.0001**

Model S3

Balanus glandula recruit year 1 abundance ~ treatment_{y1} + (1|block)
Error distribution: Quasi-Poisson

Table S9. Model summary table for Model S3, a generalized linear mixed effects model of *B. glandula* recruit abundance on experimental tiles during peak recruitment in the first year of the thermal manipulation. Recruit abundance was modeled as a function of the temperature treatment, with a random effect of block. Coefficients given are relative to the cool treatment, and the model was tested using a Type II ANOVA. Treatment_{y1} = treatment in year one, SE = standard error, df = degrees of freedom

Term	Coefficient	SE	χ^2	df	*P*
Intercept	4.984	0.326			
Treatment_{y1}	0.0899	0.0769	1.37	1	0.243

Model S4

Chthamalus dalli recruit year 1 abundance ~ $treatment_{y1}$ + (1|block)
Error distribution: Quasi-Poisson

Table S10. Model summary table for Model S4, a generalized linear mixed effects model of *C. dalli* recruit abundance on experimental tiles during peak recruitment in the first year of the thermal manipulation (June 2019). Recruit abundance was modeled in relation to the temperature treatment applied in year one, with a random effect of block Coefficients given are relative to the cool treatment, and the model was tested using a Type II ANOVA. $Treatment_{y1}$ = treatment in year one, SE = standard error, df = degrees of freedom

Term	Coefficient	SE	χ^2	df	*P*
Intercept	1.692	0.303			
$Treatment_{y1}$	-0.469	0.231	4.13	1	**0.0422**

Model S5

Balanus glandula recruit year 2 abundance ~ $treatment_{y1}$ * $treatment_{y2}$ + (1|block)
Error distribution: Quasi-Poisson

Table S11. Model summary table for Model S4, a generalized linear mixed effects model of *B. glandula* recruit abundance on experimental tiles during peak recruitment in the first year of the thermal manipulation (May 2019). Recruit abundance was modeled as an interaction of the temperature treatment applied in year one and the temperature treatment applied in year two, with a random effect of block. Coefficients given are relative to the cool treatment, and the model was tested using a Type III ANOVA. $Treatment_{y1}$ = treatment in year one, $treatment_{y2}$ = treatment in year two, SE = standard error, df = degrees of freedom

Term	Coefficient	SE	χ^2	df	*P*
Intercept	4.934	0.159			
$Treatment_{y1}$	-0.3884	0.1576	6.07	1	**0.0138**
$Treatment_{y2}$	-1.301	0.210	38.34	1	**$5.94x10^{-10}$**
$Treatment_{y1}$ * $Treatment_{y2}$	0.3537	0.2900	1.49	1	0.223

Table S12. Tukey-Kramer *post hoc* comparison of *B. glandula* recruitment between treatment groups in year two of the thermal manipulation. See Table S3 for treatment codes and abbreviations.

Contrast	Estimate	SE	df	*z* ratio	*P*
CC–WC	0.388	0.158	Inf	2.46	0.0657
CC–CW	1.301	0.210	Inf	6.19	**<0.0001**
CC–WW	1.335	0.193	Inf	6.91	**<0.0001**
WC–CW	0.912	0.220	Inf	4.15	**0.0002**
WC–WW	0.947	0.206	Inf	4.60	**<0.0001**
CW–WW	0.035	0.242	Inf	0.14	0.999

Model S6

Chthamalus dalli recruit year 2 abundance ~ treatment_{y1} * treatment_{y2} + (1|block)
Error distribution: Quasi-Poisson

Table S13. Model summary table for Model S6, a generalized linear mixed effects model of *B. glandula* recruit abundance on experimental tiles during peak recruitment in the first year of the thermal manipulation. Recruit abundance was modeled as an interaction of the temperature treatment applied in year one and the temperature treatment applied in year two, with a random effect of block. Coefficients given are relative to the cool treatment, and the model was tested using a Type III ANOVA. Treatment_{y1} = treatment in year one, treatment_{y2} = treatment in year two, SE = standard error, df = degrees of freedom

Term	Coefficient	SE	χ^2	df	*P*
Intercept	3.347	0.208			
Treatment_{y1}	-0.392	0.166	5.56	1	**0.0184**
Treatment_{y2}	-0.852	0.195	19.16	1	**1.20×10^{-5}**
Treatment_{y1} * Treatment_{y2}	0.430	0.272	2.50	1	0.114

Table S14. Tukey-Kramer *post hoc* comparison of *C. dalli* recruitment between treatment groups in year two of the thermal manipulation. See Table S3 for treatment codes and abbreviations.

Contrast	Estimate	SE	df	*z* ratio	*P*
CC–WC	0.392	0.158	Inf	2.36	0.0856
CC–CW	0.852	0.195	Inf	4.38	**0.0001**
CC–WW	0.815	0.178	Inf	4.58	**<0.0001**
WC–CW	0.460	0.208	Inf	2.22	0.119
WC–WW	0.423	0.192	Inf	2.20	0.124
CW–WW	-0.038	0.215	Inf	-0.18	0.998

Model S7

Balanus glandula year 1 adult abundance ~ $treatment_{y1}$ + (1|block)
Error distribution: Quasi-Poisson

Table S15. Model summary table for Model S7, a generalized linear mixed effects model of adult *B. glandula* abundance on experimental tiles at the end of the first year of the thermal manipulation. Barnacle abundance was modeled in relation to the temperature treatment applied in year one, with a random effect of block. Coefficients given are relative to the cool treatment, and the model was tested using a Type II ANOVA. $Treatment_{y1}$ = treatment in year one, SE = standard error, df = degrees of freedom

Term	Coefficient	SE	χ^2	df	*P*
Intercept	3.237	0.275			
$Treatment_{y1}$	-1.524	0.148	106.20	1	**$<2.2x10^{-16}$**

Model S8

Balanus glandula year 2 adult abundance ~ treatment_{y1} * treatment_{y2} + (1|block)
Error distribution: Quasi-Poisson

Table S16. Model summary table for Model S8, a generalized linear mixed effects model of adult *B. glandula* abundance on experimental tiles at the end of the second year of the thermal manipulation. Barnacle abundance was modeled as an interaction of the temperature treatment applied in year one and the temperature treatment applied in year two, with a random effect of block. Coefficients given are relative to the cool treatment, and the model was tested using a Type III ANOVA. Treatment_{y1} = treatment in year one, treatment_{y2} = treatment in year two, SE = standard error, df = degrees of freedom

Term	Coefficient	SE	χ^2	df	*P*
Intercept	3.487	0.379			
Treatment_{y1}	-0.822	0.477	2.97	1	0.0846
Treatment_{y2}	-0.807	0.505	2.55	1	0.110
Treatment_{y1} * Treatment_{y2}	0.156	0.715	0.048	1	0.827

Table S17. Tukey-Kramer *post hoc* comparison of adult *B. glandula* abundance between treatment groups in year two of the thermal manipulation. See Table S3 for treatment codes and abbreviations.

Contrast	Estimate	SE	df	*z* ratio	*P*
CC–WC	0.822	0.477	Inf	1.73	0.311
CC–CW	0.807	0.505	Inf	1.60	0.380
CC–WW	1.473	0.478	Inf	3.08	**0.0111**
WC–CW	-0.016	0.551	Inf	-0.028	1.00
WC–WW	0.651	0.525	Inf	1.24	0.601
CW–WW	0.666	0.535	Inf	1.25	0.598

Model S9

Balanus glandula mortality (%) ~ $treatment_{y1}$ + (1|block/number)
Error distribution: Tweedie

Table S18. Model summary table for Model S9, a generalized linear mixed effects model of *B. glandula* mortality on experimental tiles on 27 August 2019, during the first year of the thermal manipulation. Barnacle abundance was modeled in relation to the temperature treatment applied in year one, with a random effect of individual tile. Coefficients given are relative to the cool treatment, and the model was tested using a Type II ANOVA. $Treatment_{y1}$ = treatment in year one, SE = standard error, df = degrees of freedom

Term	Coefficient	SE	χ^2	df	*P*
Intercept	2.367	0.314			
$Treatment_{y1}$	1.573	0.275	32.63	1	**1.11×10^{-8}**

Model S10

Balanus glandula mortality (%) ~ $treatment_{y1}$ * $treatment_{y2}$ + date + (1|block/number)
Error distribution: Tweedie

Table S19. Model summary table for Model S10, a generalized linear mixed effects model of adult *C. dalli* abundance on experimental tiles at the end of the second year of the thermal manipulation. Barnacle abundance was modeled as an interaction of the temperature treatment applied in year one and the temperature treatment applied in year two plus an additive term for sampling date, with a random effect of block. Coefficients given are relative to the consistently cool treatment, and the model was tested using a Type III ANOVA. $Treatment_{y1}$ = treatment in year one, $treatment_{y2}$ = treatment in year two, SE = standard error, df = degrees of freedom

Term	Coefficient	SE	χ^2	df	*P*
Intercept	0.992	0.355			
$Treatment_{y1}$	-0.082	0.460	0.03	1	0.859
$Treatment_{y2}$	1.556	0.440	12.48	1	**$4.12x10^{-4}$**
Date: 2020-09-14	0.169	0.219	1.07	2	0.585
Date: 2020-12-11	0.216	0.316			
$Treatment_{y1}$ * $Treatment_{y2}$	-1.471	0.663	4.93	1	**0.0264**

Model S11

Log (*Balanus glandula* basal diameter) ~ treatment_{y1} + (1|block/number)
Error distribution: Gaussian

Table S20. Model summary table for Model S11, a generalized linear mixed effects model of *B. glandula* size on experimental tiles on 27 August 2019, during the first year of the thermal manipulation. Barnacle abundance was modeled in relation to the temperature treatment applied in year one, with a random effect of individual tile. Coefficients given are relative to the cool treatment, and the model was tested using a Type II ANOVA. Treatment_{y1} = treatment in year one, SE = standard error, df = degrees of freedom

Term	Coefficient	SE	F	df	df (residuals)	*P*
Intercept	1.519	0.029				
Treatment_{y1}	-0.349	0.050	25.09	1	98	**2.41×10^{-6}**

Model S12

Log (*Balanus glandula* basal diameter) ~ $treatment_{y1}$ * $treatment_{y2}$ * date + (1|block/number)
Error distribution: Gaussian

Table S21. Model summary table for Model S12, a generalized linear mixed effects model of adult *B. glandula* size on experimental tiles at the end of the second year of the thermal manipulation. Barnacle size was modeled as an interaction of the temperature treatment applied in year one and the temperature treatment applied in year two and the date on which data were collected, with a random effect of block Coefficients given are relative to the cool treatment (for treatment) and tiles on 9 July 2020 (for date), and the model was tested using a Type III ANOVA. $Treatment_{y1}$ = treatment in year one, $treatment_{y2}$ = treatment in year two, SE = standard error, df = degrees of freedom

Term	Coefficient	SE	F	df	df (residuals)	*P*
Intercept	1.866	0.082				
$Treatment_{y1}$	-0.188	0.068	7.60	1	89	**0.00710**
$Treatment_{y2}$	-0.047	0.703	0.42	1	103	0.517
Date: 2020-09-14	-0.019	0.027	2.07	2	1516	0.127
Date: 2020-12-11	0.047	0.033				
$Treatment_{y1}$ * $Treatment_{y2}$	-0.336	0.105	10.21	1	83	**0.00193**
$Treatment_{y1}$ * Date: 2020-09-14	0.071	0.040	4.62	2	1518	**0.0100**
$Treatment_{y1}$ * Date: 2020-12-11	0.146	0.050				
$Treatment_{y2}$ * Date: 2020-09-14	0.028	0.048	1.01	2	1554	0.363
$Treatment_{y2}$ * Date: 2020-12-11	-0.060	0.061				
$Treatment_{y1}$ * $Treatment_{y2}$ * Date: 2020-09-14	0.246	0.066	6.92	2	1552	**0.00102**
$Treatment_{y1}$ * $Treatment_{y2}$ * Date: 2020-12-11	0.125	0.081				

Model S13

Chthamalus dalli year 1 adult abundance ~ treatment_{y1} + (1|block)
Error distribution: Quasi-Poisson

Table S22. Model summary table for Model S13, a generalized linear mixed effects model of adult *C. dalli* abundance on experimental tiles at the end of the first year of the thermal manipulation. Barnacle abundance was modeled in relation to temperature treatment applied in year one, with a random effect of block. Coefficients given are relative to the cool treatment, and the model was tested using a Type II ANOVA. Treatment_{y1} = treatment in year one, SE = standard error, df = degrees of freedom

Term	Coefficient	SE	χ^2	df	*P*
Intercept	-1.654	0.572			
Treatment_{y1}	-0.287	0.356	0.65	1	0.420

Model S14

Chthamalus dalli year 2 adult abundance ~ treatment_{y1} * treatment_{y2} + (1|block)
Error distribution: Quasi-Poisson

Table S23. Model summary table for Model S14, a generalized linear mixed effects model of adult *C. dalli* abundance on experimental tiles at the end of the second year of the thermal manipulation. Barnacle abundance was modeled as an interaction of the temperature treatment applied in year one and the temperature treatment applied in year two, with a random effect of block Coefficients given are relative to the cool treatment, and the model was tested using a Type III ANOVA. Treatment_{y1} = treatment in year one, treatment_{y2} = treatment in year two, SE = standard error, df = degrees of freedom

Term	Coefficient	SE	χ^2	df	*P*
Intercept	3.080	0.408			
Treatment_{y1}	-0.502	0.462	1.18	1	0.277
Treatment_{y2}	-0.239	0.490	0.24	1	0.626
Treatment_{y1} * Treatment_{y2}	-0.139	0.685	0.041	1	0.840

Table S24. Tukey-Kramer *post hoc* comparison of adult *C. dalli* abundance between treatment groups in year two of the thermal manipulation. See Table S3 for treatment codes and abbreviations.

Contrast	Estimate	SE	df	*z* ratio	*P*
CC–WC	0.502	0.462	Inf	1.09	0.698
CC–CW	0.239	0.490	Inf	0.49	0.962
CC–WW	0.879	0.450	Inf	1.95	0.207
WC–CW	-0.263	0.518	Inf	-0.51	0.957
WC–WW	0.377	0.487	Inf	0.77	0.866
CW–WW	0.641	0.500	Inf	1.28	0.575

Model S15

Lottia spp. abundance ~ treatment_{y1} * treatment_{y2} + (1|block)
Error distribution: Quasi-Poisson

Table S25. Model summary table for Model S15, a generalized linear mixed effects model of *Lottia* spp. abundance on experimental tiles at the end of the second summer, on 14 September 2020. Limpet abundance was modeled as an interaction of the temperature treatment applied in year one and the temperature treatment applied in year two, with a random effect of block. Coefficients for treatment are given are relative to the cool treatment, and the model was tested using a Type III ANOVA. Treatment_{y1} = treatment in year one, treatment_{y2} = treatment in year two, SE = standard error, df = degrees of freedom

Term	Coefficient	SE	χ^2	df	*P*
Intercept	0.498	0.532			
Treatment_{y1}	-0.294	0.191	2.36	1	0.124
Treatment_{y2}	-0.781	0.235	11.07	1	**8.77×10^{-4}**
Treatment_{y1} * Treatment_{y2}	0.102	0.342	0.09	1	0.766

Table S26. Tukey-Kramer *post hoc* comparison of *Lottia* spp. abundance between treatment groups at the end of summer in year two of the thermal manipulation. See Table S3 for treatment codes and abbreviations.

Contrast	Estimate	SE	df	*z* ratio	*P*
CC–WC	0.294	0.191	Inf	1.54	0.416
CC–CW	0.781	0.235	Inf	3.33	**0.0049**
CC–WW	0.973	0.236	Inf	4.12	**0.0002**
WC–CW	0.487	0.249	Inf	1.96	0.204
WC–WW	0.679	0.250	Inf	2.72	**0.0333**
CW–WW	0.192	0.284	Inf	0.676	0.906

Table S26. Model summary table for Model S15, a generalized linear mixed effects model of *Lottia* spp. abundance on experimental tiles at the end of the second winter, on 24 February 2021. Limpet abundance was modeled as an interaction of the temperature treatment applied in year one and the temperature treatment applied in year two, with a random effect of block. Coefficients for treatment are given are relative to the cool treatment, and the model was tested using a Type III ANOVA. $Treatment_{y1}$ = treatment in year one, $treatment_{y2}$ = treatment in year two, SE = standard error, df = degrees of freedom

Term	Coefficient	SE	χ^2	df	*P*
Intercept	1.733	0.528			
$Treatment_{y1}$	-0.621	0.328	3.57	1	0.0587
$Treatment_{y2}$	-0.744	0.494	2.27	1	0.132
$Treatment_{y1}$ * $Treatment_{y2}$	-1.186	0.865	1.88	1	0.170

Table S27. Tukey-Kramer *post hoc* comparison of *Lottia* spp. abundance between treatment groups at the end of the winter in year two of the thermal manipulation. See Table S3 for treatment codes and abbreviations.

Contrast	Estimate	SE	df	*z* ratio	*P*
CC–WC	0.621	0.328	Inf	1.89	0.232
CC–CW	0.744	0.494	Inf	1.51	0.434
CC–WW	2.551	0.740	Inf	3.45	**0.0032**
WC–CW	0.123	0.516	Inf	0.24	0.995
WC–WW	1.930	0.749	Inf	2.58	**0.0492**
CW–WW	1.807	0.805	Inf	2.25	0.111

Model S16

Littorina spp. abundance ~ treatment_{y1} * treatment_{y2} + (1|block)
Error distribution: Quasi-Poisson

Table S28. Model summary table for Model S16, a generalized linear mixed effects model of *Littorina* spp. abundance on experimental tiles at the end of the second summer, on 14 September 2020. Littorine abundance was modeled as an interaction of the temperature treatment applied in year one and the temperature treatment applied in year two, with a random effect of block. Coefficients given are relative to the cool treatment, and the model was tested using a Type III ANOVA. Treatment_{y1} = treatment in year one, treatment_{y2} = treatment in year two, SE = standard error, df = degrees of freedom

Term	Coefficient	SE	χ^2	df	*P*
Intercept	4.094	0.205			
Treatment_{y1}	-1.045	0.249	17.56	1	**2.79×10^{-5}**
Treatment_{y2}	-0.909	0.224	13.38	1	**2.54×10^{-4}**
Treatment_{y1} * Treatment_{y2}	0.482	0.374	1.66	1	0.198

Table S29. Tukey-Kramer *post hoc* comparison of *Littorina* spp. abundance between treatment groups at the end of summer in year two of the thermal manipulation. See Table S3 for treatment codes and abbreviations.

Contrast	Estimate	SE	df	*z* ratio	*P*
CC–WC	1.045	0.249	Inf	4.19	**0.0002**
CC–CW	0.909	0.248	Inf	3.66	**0.0014**
CC–WW	1.473	0.256	Inf	5.76	**<0.0001**
WC–CW	-0.136	0.283	Inf	-0.48	0.963
WC–WW	0.427	0.282	Inf	1.52	0.428
CW–WW	0.563	0.286	Inf	1.97	0.199

Table S30. Model summary table for Model S16, a generalized linear mixed effects model of *Littorina* spp. abundance on experimental tiles at the end of the second winter, on 24 February 2021. Limpet abundance was modeled as an interaction of the temperature treatment applied in year one and the temperature treatment applied in year two, with a random effect of block. Coefficients given are relative to the cool treatment, and the model was tested using a Type III ANOVA. $Treatment_{y1}$ = treatment in year one, $treatment_{y2}$ = treatment in year two, SE = standard error, df = degrees of freedom

Term	Coefficient	SE	χ^2	df	*P*
Intercept	2.379	0.347			
$Treatment_{y1}$	-0.916	0.505	3.29	1	0.0698
$Treatment_{y2}$	-1.159	0.589	3.87	1	**0.0491**
$Treatment_{y1}$ * $Treatment_{y2}$	-0.571	1.000	0.326	1	0.568

Table S31. Tukey-Kramer *post hoc* comparison of *Littorina* spp. abundance between treatment groups at the end of winter in year two of the thermal manipulation. See Table S3 for treatment codes and abbreviations.

Contrast	Estimate	SE	df	*z* ratio	*P*
CC–WC	0.916	0.505	Inf	1.81	0.267
CC–CW	1.159	0.589	Inf	1.97	0.200
CC–WW	2.646	0.776	Inf	3.41	**0.0036**
WC–CW	0.243	0.639	Inf	0.38	0.981
WC–WW	1.730	0.814	Inf	2.12	0.145
CW–WW	1.487	0.863	Inf	1.72	0.311

Model S17

Algal cover (%) ~ treatment + s(time) + s(time, by = treatment) + s(block, type = "re")
Error distribution: Gaussian
Correlation: AR(1) process

Table S32. Model summary table for Model S17, a generalized additive mixed model of differences in algal cover over time between treatments in the first year of the experiment (after 27 August 2019). Algal cover was modeled in relation to treatment and smoothed effects of time (days since experiment start) within each treatment, with a random effect of block and an AR(1) process to account for autocorrelation of the residuals. Estimates and differences between smooth functions are given relative to the cool treatment. SE = standard error, edf = effective degrees of freedom, W = warm treatment.

Component	Term	Estimate	SE	t	*P*
Linear	Intercept	17.241	3.043		
	Treatment: W	6.943	2.101	3.30	**0.00109**
		edf		**F**	***P***
Smooth	s(time)	1.92		29.60	**$<2x10^{-16}$**
	s(time):W	1.49		30.33	**$3.64x10^{-7}$**
	s(block)	2.68		1.12	0.0678

Model S18

Algal cover (%) ~ $treatment_{y1}$ * $treatment_{y2}$ + s(time) + s(time, by = treatment)
+ s(block, type = "re")
Error distribution: Gaussian
Correlation: AR(1) process

Table S33. Model summary table for Model S18, a generalized additive mixed model of differences in algal cover over time between treatments in the second year of the experiment. Algal cover was modeled in relation to the interactive effect of treatment in year one and treatment in year two and smoothed effects of time (days since the experiment start) within each treatment, with a random effect of block and an AR(1) process to account for autocorrelation of the residuals. Estimates and differences between smooth functions are given relative to the cool treatment. k=5 for smoothing functions of time. $Treatment_{y1}$ = treatment in year one, $treatment_{y2}$ = treatment in year two, SE = standard error, edf = effective degrees of freedom. See Table S3 for treatment codes.

Component	Term	Estimate	SE	t	*P*
Linear	Intercept	2.456	1.135		
	$Treatment_{y1}$	1.322	1.077	1.23	0.220
	$Treatment_{y2}$	3.116	1.141	2.73	**0.00656**
	$Treatment_{y1}$ * $Treatment_{y2}$	-3.867	1.504	-2.57	**0.0104**
		edf		**F**	***P***
Smooth	s(time)	3.73		6.57	**0.00466**
	s(time):CW	3.44		5.88	**0.00204**
	s(time):WC	2.40		9.12	**4×10^{-5}**
	s(time):WW	1.00		3.71	0.0548
	s(block)	0.40		0.09	0.361

Model S19

Species richness ~ $treatment_{y1}$ + (1|block)
Error distribution: Poisson

Table S34. Model summary table for Model S19, a generalized linear mixed effects model of the species richness on experimental tile communities at the end of the first summer, on 20 October 2019. Species richness was modeled under a Poisson distribution as a function of treatment, with block included as a random intercept effect. Coefficients given are relative to the cool treatment, and the model was tested using a Type II ANOVA. $Treatment_{y1}$ = treatment in year one, SE = standard error, df = degrees of freedom.

Term	Coefficient	SE	χ^2	df	*P*
Intercept	1.386	0.083			
$Treatment_{y1}$	-0.468	0.116	16.33	1	**5.32×10^{-5}**

Table S35. Model summary table for Model S19, a generalized linear mixed effects model of the species richness on experimental tile communities at the end of the first winter, on 15 March 2020. Species richness was modeled under a Poisson distribution as a function of treatment, with block included as a random intercept effect. Coefficients given are relative to the cool treatment, and the model was tested using a Type II ANOVA. $Treatment_{y1}$ = treatment in year one, SE = standard error, df = degrees of freedom.

Term	Coefficient	SE	χ^2	df	*P*
Intercept	1.138	0.189			
$Treatment_{y1}$	-0.959	0.111	74.85	1	**$<2.2 \times 10^{-16}$**

Model S20

Log(Species richness + 1) ~ treatment_{y1} * treatment_{y2} + (1|block)
Error distribution: Gaussian

Table S36. Model summary table for Model S20, a linear mixed effects model of the species richness of experimental tiles at the end of the second summer, on 14 September 2020. Species richness was log-transformed and modeled under a normal distribution in relation to the interaction of treatments in year one and year two, with block included as a random effect. Coefficients given are relative to the cool treatment, and the model was tested using a Type III ANOVA. Treatment_{y1} = treatment in year one, treatment_{y2} = treatment in year two, SE = standard error, df = degrees of freedom.

Term	Coefficient	SE	χ^2	df	*P*
Intercept	1.814	0.044			
Treatment_{y1}	-0.078	0.061	1.61	1	0.204
Treatment_{y2}	-0.137	0.063	4.73	1	**0.0297**
Treatment_{y1} * Treatment_{y2}	-0.065	0.086	0.57	1	0.450

Table S37. Tukey-Kramer *post hoc* comparison of species richness between treatment groups at the end of summer in year two of the thermal manipulation. See Table S3 for treatment codes and abbreviations.

Contrast	Estimate	SE	df	t ratio	*P*
CC–WC	0.078	0.061	78	1.22	0.585
CC–CW	0.137	0.063	78	2.17	0.140
CC–WW	0.280	0.059	78	4.78	**<0.001**
WC–CW	0.059	0.064	78	0.93	0.790
WC–WW	0.202	0.059	78	3.42	**0.0054**
CW–WW	0.143	0.061	78	2.35	0.0967

Model S21

Species richness ~ treatment_{y1} * treatment_{y2} + (1|block)
Error distribution: Gaussian

Table S38. Model summary table for Model S21, a generalized linear mixed effects model of the species richness of experimental tiles at the end of the second winter, on 24 February 2021. Species richness was modeled under a Poisson distribution in relation to the interaction of treatments in year one and year two, with block included as a random effect. Coefficients given are relative to the cool treatment, and the model was tested using a Type III ANOVA. Treatment_{y1} = treatment in year one, treatment_{y2} = treatment in year two, SE = standard error, df = degrees of freedom.

Term	Coefficient	SE	χ^2	df	*P*
Intercept	1.655	0.180			
Treatment_{y1}	-0.106	0.185	0.33	1	0.566
Treatment_{y2}	-0.300	0.228	1.73	1	0.188
Treatment_{y1} * Treatment_{y2}	-0.417	0.312	1.79	1	0.181

Table S39. Tukey-Kramer *post hoc* comparison of species richness between treatment groups at the end of winter in year two of the thermal manipulation. See Table S3 for treatment codes and abbreviations.

Contrast	Estimate	SE	df	*z* ratio	*P*
CC–WC	0.106	0.185	Inf	0.57	0.940
CC–CW	0.300	0.228	Inf	1.32	0.552
CC–WW	0.824	0.213	Inf	3.87	**0.0006**
WC–CW	0.194	0.233	Inf	0.83	0.839
WC–WW	0.717	0.219	Inf	3.27	**0.0059**
CW–WW	0.524	0.250	Inf	2.09	0.156

Model S22

Invertebrate Shannon diversity ~ $treatment_{y1}$ + (1|block)
Error distribution: Tweedie
Dispersion formula: ~ $treatment_{y1}$

Table S40. Model summary table for Model S22, a generalized linear mixed effects model of the invertebrate Shannon diversity of experimental tile communities at the end of the first summer, on 20 October 2019. Invertebrate Shannon diversity was modeled under a Tweedie distribution in relation to the treatment in year one, with block included as a random effect. Coefficients given are relatie to the cool treatment, and the model was tested using a Type II ANOVA. $Treatment_{y1}$ = treatment in year one, $treatment_{y2}$ = treatment in year two, SE = standard error, df = degrees of freedom.

Term	Coefficient	SE	χ^2	df	*P*
Intercept	-1.017	0.115			
$Treatment_{y1}$	-0.085	0.244	0.122	1	0.727
Dispersion model					
Intercept	-1.505	0.162			
$Treatment_{y1}$	1.363	0.181			

Table S41. Model summary table for Model S22, a generalized linear mixed effects model of the invertebrate Shannon diversity of experimental tile communities at the end of the first winter, on 15 March 2020. Invertebrate Shannon diversity was modeled under a Tweedie distribution in relation to the treatment in year one, with block included as a random effect. Coefficients given are relatie to the cool treatment, and the model was tested using a Type II ANOVA. See Table S3 for abbreviations.

Term	Coefficient	SE	χ^2	df	*P*
Intercept	-1.351	0.425			
$Treatment_{y1}$	-1.401	0.271	26.67	1	**2.41×10^{-7}**
Dispersion model					
Intercept	-1.500	0.075			
$Treatment_{y1}$	0.987	0.098			

Model S23

Invertebrate Shannon diversity ~ treatment_{y1} * treatment_{y2} + (1|block)
Error distribution: Tweedie

Table S42. Model summary table for Model S23, a generalized linear mixed effects model of the invertebrate Shannon diversity of experimental tiles at the end of the second summer, on 14 September 2020. Invertebrate Shannon diversity was modeled under a Tweedie distribution in relation to the interaction of treatments in year one and year two, with block included as a random effect. Coefficients given are relative to the cool treatment, and the model was tested using a Type III ANOVA. Treatment_{y1} = treatment in year one, treatment_{y2} = treatment in year two, SE = standard error, df = degrees of freedom.

Term	Coefficient	SE	χ^2	df	*P*
Intercept	1.200	0.054			
Treatment_{y1}	-0.200	0.074	7.35	1	**0.00669**
Treatment_{y2}	-0.109	0.076	2.07	1	0.150
Treatment_{y1} * Treatment_{y2}	-0.010	0.104	0.0097	1	0.921

Table S43. Tukey-Kramer *post hoc* comparison of invertebrate Shannon diversity between treatment groups at the end of the second summer of the thermal manipulation. See Table S3 for treatment codes and abbreviations.

Contrast	Estimate	SE	df	t ratio	*P*
CC–WC	0.200	0.074	78	2.71	**0.0402**
CC–CW	0.109	0.076	78	1.44	0.479
CC–WW	0.319	0.070	78	4.56	**0.0001**
WC–CW	-0.090	0.077	78	-1.18	0.642
WC–WW	0.119	0.071	78	1.69	0.338
CW–WW	0.210	0.073	78	2.88	**0.0261**

Table S44. Model summary table for Model S23, a generalized linear mixed effects model of the invertebrate Shannon diversity of experimental tiles at the end of the second winter, on 24 February 2021. Invertebrate Shannon diversity was modeled under a Tweedie distribution in relation to the interaction of treatments in year one and year two, with block included as a random effect. Coefficients given are relative to the cool treatment, and the model was tested using a Type III ANOVA. $Treatment_{y1}$ = treatment in year one, $treatment_{y2}$ = treatment in year two, SE = standard error, df = degrees of freedom.

Term	Coefficient	SE	χ^2	df	*P*
Intercept	0.964	0.139			
$Treatment_{y1}$	-0.318	0.169	3.52	1	0.0605
$Treatment_{y2}$	-0.214	0.189	1.28	1	0.258
$Treatment_{y1}$ * $Treatment_{y2}$	-0.046	0.245	0.04	1	0.851

Table S45. Tukey-Kramer *post hoc* comparison of invertebrate Shannon diversity between treatment groups at the end of the second winter of the thermal manipulation. See Table S3 for treatment codes and abbreviations.

Contrast	Estimate	SE	df	t ratio	*P*
CC–WC	0.318	0.169	41	1.88	0.254
CC–CW	0.214	0.189	41	1.13	0.673
CC–WW	0.578	0.159	41	3.62	**0.0042**
WC–CW	-0.104	0.190	41	-0.55	0.947
WC–WW	0.260	0.161	41	1.61	0.383
CW–WW	0.364	0.177	41	2.05	0.186

Model S24

Algal Shannon diversity ~ $treatment_{y1}$ + (1|block)
Error distribution: Tweedie

Table S46. Model summary table for Model S24, a generalized linear mixed effects model of the algal Shannon diversity of experimental tile communities for data collected at the end of the first winter, on 15 March 2020. Algal Shannon diversity was modeled under a Tweedie distribution as a function of treatment during the first year, with block included as a random intercept effect. Coefficients given are relative to the cool treatment, and the model was tested using a Type II ANOVA. $Treatment_{y1}$ = treatment in year one, SE = standard error, df = degrees of freedom.

Term	Coefficient	SE	χ^2	df	*P*
Intercept	-2.507	0.651			
$Treatment_{y1}$	-1.855	0.602	9.48	1	**0.00208**

Model S25

Algal Shannon diversity ~ $treatment_{y1}$ * $treatment_{y2}$ + (1|block)
Error distribution: Tweedie

Table S47. Model summary table for Model S25, a generalized linear mixed effects model of the algal Shannon diversity of experimental tiles at the end of the second winter, on 24 February 2021. Algal Shannon diversity was modeled under a Tweedie distribution in relation to the interaction of treatments in year one and year two, with block included as a random effect. Coefficients given are relative to the cool treatment, and the model was tested using a Type III ANOVA. $Treatment_{y1}$ = treatment in year one, $treatment_{y2}$ = treatment in year two, SE = standard error, df = degrees of freedom.

Term	Coefficient	SE	χ^2	df	*P*
Intercept	-1.609	0.507			
$Treatment_{y1}$	0.7698	0.6407	1.444	1	0.230
$Treatment_{y2}$	-0.3348	0.8722	0.147	1	0.701
$Treatment_{y1}$ * $Treatment_{y2}$	-1.105	1.114	0.984	1	0.321

Table S48. Tukey-Kramer *post hoc* comparison of algal Shannon diversity between treatment groups at the end of winter in year two of the thermal manipulation. See Table S3 for treatment codes and abbreviations.

Contrast	Estimate	SE	df	z ratio	*P*
CC–WC	-0.770	0.641	Inf	-1.20	0.626
CC–CW	0.335	0.872	Inf	0.38	0.981
CC–WW	0.670	0.765	Inf	0.88	0.818
WC–CW	1.105	0.810	Inf	1.35	0.522
WC–WW	1.440	0.693	Inf	2.08	0.161
CW–WW	0.335	0.912	Inf	0.37	0.983

Model S26

Species assemblage ~ $treatment_{y1}$ * $treatment_{y2}$

Table S49. Model summary table of PERMANOVA output for Model S26 describing differences in epifaunal community composition of experimental tiles destructively sampled on 14 September 2020. PERMANOVA used constrained ordination within experimental blocks via distance-based redundancy analyses with Bray-Curtis distances. Community structure was modeled in relation the interaction of treatment of year one and treatment in year two. $Treatment_{y1}$ = treatment in year one, $treatment_{y2}$ = treatment in year two, df = degrees of freedom.

Term	df	Sum of squares	F	*P*
$Treatment_{y1}$	1	0.434	1.69	0.0825
$Treatment_{y2}$	1	0.389	1.51	0.120
$Treatment_{y1}$ * $Treatment_{y2}$	1	0.329	1.28	0.192
Residuals	31	7.952		

Table S50. Multiple pairwise comparisons of epifaunal community composition across treatments using constrained ordination via distance-based redundancy analyses with Bray-Curtis distances. Epifauna were destructively sampled on 14 September 2020. See Table S3 for treatment codes and abbreviations.

Comparison	df	Sum of squares	F	*P*
CC – CW	1	0.283	1.20	0.280
CC – WC	1	0.288	1.25	0.246
CC – WW	1	0.777	2.68	**0.018**
CW – WC	1	0.047	0.21	0.990
CW – WW	1	0.454	1.59	0.159
WC – WW	1	0.435	1.58	0.138

Table S51. Model summary table of PERMANOVA output for Model S26 describing differences in epifaunal community composition of experimental tiles destructively sampled on 24 February 2021. PERMANOVA used constrained ordination within experimental blocks via distance-based redundancy analyses with Bray-Curtis distances. Community structure was modeled in relation the interaction of treatment of year one and treatment in year two. $Treatment_{y1}$ = treatment in year one, $treatment_{y2}$ = treatment in year two, df = degrees of freedom.

Term	df	Sum of squares	F	*P*
$Treatment_{y1}$	1	0.674	2.39	**0.0141**
$Treatment_{y2}$	1	1.030	3.66	**0.0015**
$Treatment_{y1}$ * $Treatment_{y2}$	1	0.626	2.22	**0.0125**
Residuals	37	10.410		

Table S52. Multiple pairwise comparisons of epifaunal community composition across treatments using constrained ordination via distance-based redundancy analyses with Bray-Curtis distances. Epifauna were destructively sampled on 24 February 2021. See Table S3 for treatment codes and abbreviations.

Comparison	df	Sum of squares	F	*P*
CC – CW	1	0.834	3.34	**0.003**
CC – WC	1	0.617	2.29	**0.017**
CC – WW	1	1.600	5.74	**0.001**
CW – WC	1	0.111	0.39	0.942
CW – WW	1	0.486	1.64	0.147
WC – WW	1	0.821	2.69	**0.005**

Model S27

Species assemblage heterogeneity ~ treatment

Table S53. Model summary table of PERMDISP output for Model S27 of differences in epifaunal community composition heterogeneity of experimental tiles destructively sampled in September 2020. df = degrees of freedom.

Term	df	Sum of squares	Mean squares	F	*P*
Treatment	3	0.0714	0.0238	2.58	0.0714
Residuals	31	0.2862	0.0092		

Table S54. Model summary table of PERMDISP output for Model S27 of differences in epifaunal community composition heterogeneity of experimental tiles destructively sampled in February 2021. df = degrees of freedom.

Variable	df	Sum of squares	Mean squares	F	*P*
Treatment	3	0.0440	0.0147	0.946	0.428
Residuals	37	0.5732	0.0155		

Model S28

Species richness ~ $treatment_{y1}$ * $treatment_{y2}$ + (1 | block)
Error distribution: Poisson

Table S55. Model summary table for Model S28, a generalized linear mixed effects model of the species richness of epifauna from destructively sampled tile communities collected on 14 September 2020. Species richness was modeled under a Poisson distribution in relation to the interaction of treatments in year one and year two, with block included as a random effect. Coefficients given are relative to the cool treatment, and the model was tested using a Type III ANOVA. $Treatment_{y1}$ = treatment in year one, $treatment_{y2}$ = treatment in year two, df = degrees of freedom.

Term	Coefficient	SE	χ^2	df	*P*
Intercept	2.291	0.106			
$Treatment_{y1}$	-0.107	0.154	0.48	1	0.489
$Treatment_{y2}$	-0.244	0.165	2.17	1	0.141
$Treatment_{y1}$ * $Treatment_{y2}$	-0.187	0.243	0.59	1	0.442

Table S56. Tukey-Kramer *post hoc* comparison of species richness of epifauna from destructively sampled tile communities between treatment groups at the end of the second summer of the thermal manipulation. See Table S3 for treatment codes and abbreviations.

Contrast	Estimate	SE	df	z ratio	*P*
CC–WC	0.107	0.154	Inf	0.69	0.900
CC–CW	0.244	0.165	Inf	1.47	0.454
CC–WW	0.537	0.175	Inf	3.08	**0.0112**
WC–CW	0.137	0.169	Inf	0.81	0.850
WC–WW	0.431	0.178	Inf	2.42	0.0736
CW–WW	0.294	0.188	Inf	1.56	0.401

Table S57. Model summary table for Model S28, a generalized linear mixed effects model of the species richness of epifauna from destructively sampled tile communities collected on 24 February 2021. Species richness was modeled under a Poisson distribution in relation to the interaction of treatments in year one and year two, with block included as a random effect. Coefficients given are relative to the cool treatment, and the model was tested using a Type III ANOVA. $Treatment_{y1}$ = treatment in year one, $treatment_{y2}$ = treatment in year two, df = degrees of freedom.

Term	Coefficient	SE	χ^2	df	*P*
Intercept	2.423	0.120			
$Treatment_{y1}$	-0.258	0.135	3.64	1	0.0565
$Treatment_{y2}$	-0.316	0.168	3.55	1	0.0595
$Treatment_{y1}$ * $Treatment_{y2}$	-0.161	0.233	0.48	1	0.488

Table S58. Tukey-Kramer *post hoc* comparison of species richness of epifauna from destructively sampled tile communities between treatment groups at the end of the second winter of the thermal manipulation. See Table S3 for treatment codes and abbreviations.

Contrast	Estimate	SE	df	z ratio	*P*
CC–WC	0.259	0.135	Inf	1.91	0.225
CC–CW	0.316	0.167	Inf	1.89	0.235
CC–WW	0.735	0.158	Inf	4.66	**<0.0001**
WC–CW	0.058	0.171	Inf	0.34	0.987
WC–WW	0.477	0.164	Inf	2.90	**0.0193**
CW–WW	0.420	0.187	Inf	2.25	0.111

Model S29
Shannon diversity ~ treatment_{y1} * treatment_{y2} + (1 | block)
Error distribution: Gaussian

Table S59. Model summary table for Model S29, a generalized linear mixed effects model of the Shannon diversity of epifauna from destructively sampled tile communities collected on 14 September 2020. Shannon diversity was modeled under a Tweedie distribution in relation to the interaction of treatments in year one and year two, with block included as a random effect. Coefficients given are relative to the cool treatment, and the model was tested using a Type III ANOVA. Treatment_{y1} = treatment in year one, treatment_{y2} = treatment in year two, df = degrees of freedom.

Term	Coefficient	SE	χ^2	df	*P*
Intercept	1.358	0.116			
Treatment_{y1}	-0.061	0.165	0.14	1	0.710
Treatment_{y2}	-0.248	0.170	2.14	1	0.144
Treatment_{y1} * Treatment_{y2}	-0.346	0.236	2.14	1	0.144

Table S60. Tukey-Kramer *post hoc* comparison of the Shannon diversity of epifauna from destructively sampled tile communities between treatment groups in year two of the thermal manipulation. See Table S3 for treatment codes and abbreviations.

Contrast	Estimate	SE	df	z ratio	*P*
CC–WC	0.061	0.165	29	0.372	0.982
CC–CW	0.248	0.170	29	1.46	0.472
CC–WW	0.655	0.165	29	3.98	**0.0023**
WC–CW	0.187	0.170	29	1.10	0.691
WC–WW	0.594	0.165	29	3.61	**0.0060**
CW–WW	0.407	0.170	29	2.40	0.100

Table S61. Model summary table for Model S29, a generalized linear mixed effects model of the Shannon diversity of epifauna from destructively sampled tile communities collected on 24 February 2021. Shannon diversity was modeled under a Tweedie distribution in relation to the interaction of treatments in year one and year two, with block included as a random effect. Coefficients given are relative to the cool treatment, and the model was tested using a Type III ANOVA. $Treatment_{y1}$ = treatment in year one, $treatment_{y2}$ = treatment in year two, df = degrees of freedom.

Term	Coefficient	SE	χ^2	df	*P*
Intercept	1.546	0.195			
$Treatment_{y1}$	-0.251	0.199	1.58	1	0.208
$Treatment_{y2}$	-0.179	0.233	0.59	1	0.443
$Treatment_{y1}$ * $Treatment_{y2}$	-0.472	0.305	2.40	1	0.121

Table S62. Tukey-Kramer *post hoc* comparison of the Shannon diversity of epifauna from destructively sampled tile communities between treatment groups in year two of the thermal manipulation. See Table S3 for treatment codes and abbreviations.

Contrast	Estimate	SE	df	z ratio	*P*
CC–WC	0.251	0.199	35	1.26	0.595
CC–CW	0.179	0.233	35	0.767	0.869
CC–WW	0.902	0.200	35	4.50	**0.0004**
WC–CW	-0.072	0.228	35	-0.32	0.989
WC–WW	0.651	0.199	35	3.28	**0.0121**
CW–WW	0.732	0.227	35	3.18	**0.0154**